NON-LINEAR BEHAVIOR OF CYLINDRICAL SHELLS

Thesis for the Degree of Ph. D.

MICHIGAN STATE UNIVERSITY

Cary Kau-Kei Mak

1965

This is to certify that the

thesis entitled

NON-LINEAR BEHAVIOR OF CYLINDRICAL SHELLS

presented by

Cary Kau-Kei Mak

has been accepted towards fulfillment
of the requirements for

Ph. D. degree in Civil Engineering

R. K. Wen
Major professor

Date Nov. 17, 1965

O-169

NON-LINEAR [illegible]

[illegible]

[illegible]

[illegible] the shell. The longitudinal law [illegible]

ABSTRACT

NON-LINEAR BEHAVIOR OF CYLINDRICAL SHELLS

by Cary Kau-Kei Mak

An analytical method has been developed to study the non-linear behavior of elastic thin circular cylindrical shells undergoing large displacements. The shells are supported by flexible beams on the longitudinal edges and rollers on the curved edges, or by rollers on all the edges. Three types of loading are considered: a uniform radial pressure, a uniform live load (vertical load distributed over the horizontal projection of the shell), and a uniform dead load (vertical load distributed over the curved surface of the shell).

The method of analysis is based on a large deflection theory of shells by including the quadratic terms $\left(\frac{\partial w}{\partial x}\right)^2$ and $\left(\frac{\partial w}{R\partial \phi}\right)^2$ in the strain tensor. The variational problem resulting from an application of the principle of stationary potential energy is solved approximately by the method of Rayleigh-Ritz. The radial displacement function w, with two undetermined parameters, is chosen to represent a first harmonic approximation of the deflection of the shell. The longitudinal and circumferential displacement

functions u and v, are considered to consist of two parts: u_p, v_p and u_h, v_h. The functions u_p and v_p are chosen to be the particular solutions of the equations of equilibrium in the longitudinal and circumferential directions, respectively, and u_h and v_h are homogeneous solutions of $\nabla^4 u_h = \nabla^4 v_h = 0$, so that the sums $u = u_p + u_h$ and $v = v_p + v_h$ satisfy approximately the geometric and natural boundary conditions. By applying these approximating functions to the Rayleigh-Ritz procedure, a set of two simultaneous algebraic cubic equations are obtained. With the use of a high speed digital computer, these equations are solved by the iteration scheme of Newton-Raphson. For a given shell and loading type, a load-deflection curve is obtained from a series of solutions corresponding to a range of loading intensity. The curve, in general, is non-linear. It is indicated that after a certain range of essentially linear behavior,, the stiffness of the shell decreases. In many cases the shell "buckles," i. e., the displacement would increase substantially with little change in load.

By a repeated application of the above procedure for different values of shell parameters, a number of load deflection curves are obtained. From these numerical results, the principle findings may be summarized as follows:

Among the three loading conditions considered, the shell has the lowest stiffness (or buckling load) under the dead load. The shells have lower stiffnesses or buckling loads for smaller values of the opening angle ϕ_k, smaller values of the radius to length parameter S, larger values of the radius to thickness parameter Z, and for smaller edge beams.

NON-LINEAR BEHAVIOR OF CYLINDRICAL SHELLS

By

Cary Kau-Kei Mak

A THESIS

Submitted to
Michigan State University
in partial fulfillment of the requirements
for the degree of

DOCTOR OF PHILOSOPHY

Department of Civil and Sanitary Engineering

1965

g 38040
7-7-66

ACKNOWLEDGMENTS

This report constitutes the author's doctoral dissertation, written under the direction of Dr. Robert K. L. Wen, Associate Professor of Civil Engineering, whose valuable guidance and stimulating suggestions during the course of this study is gratefully acknowledged.

The author wishes to express his thanks to Dr. C. E. Cutts, Chairman of the Department of Civil Engineering, for his encouragement and interest during the course of the author's graduate studies, to Dr. L. E. Malvern, Professor of Metallurgy, Mechanics and Material Science, and Dr. J. S. Frame, Professor of Mathematics, for their valuable suggestions in solving the non-linear equations. Also, special thanks are extended to the National Science Foundation and to the Division of Engineering Research, Michigan State University for their financial support which made this work possible.

In addition, the author wishes to extend his sincere appreciation to Dr. B. N. Beyleryan, former Research Assistant in Civil Engineering, for his assistance in checking some of the numerical computation and in obtaining computer solutions from the computer laboratory during the author's absence from Michigan State University.

And last, but not least, go thanks to the author's wife, Leonora, whose encouragement during many difficult periods is genuinely appreciated.

TABLE OF CONTENTS

LIST OF FIGURES

LIST OF APPENDICES

I. INTRODUCTION

1.1. Object and Scope

The purpose of this study is to investigate analytically the non-linear behavior of thin circular cylindrical shell panels undergoing large deflections. The objectives of this investigation were:

(1) To develop a procedure of analysis to solve the large deflection problem of cylindrical shell panels with certain boundary and loading conditions that have not been considered thus far.

(2) To apply the procedure to investigate the influences of different types of loading and of various shell parameters on the behavior of the shell structure.

This study is based on a large deflection theory advanced by Donnell (4), (1934)* who developed the non-linear equations of cylindrical shells by including certain quadratic terms in the strain-displacement relations. This approach leads to three non-linear partial differential equations of equilibrium in terms of the displacement u (in the longitudinal direction, x), v (in the circumferential direction, ϕ), and w (in the radial direction, z).

In the particular case when the loads are applied in the radial

*Numbers in the first and second parentheses refer to reference number and year of publication, respectively, as listed in the bibliography.

direction and/or on the boundary only, the equilibrium equations in x and ϕ directions can be satisfied identically by the introduction of an Airy stress function ψ. Thus the problem becomes simplified appreciably as the three equilibrium equations are reduced to one equilibrium equation in the z direction and a compatibility equation in terms of w and ψ. These two equations, being non-linear in w, are usually solved approximately either by means of the Rayleigh-Ritz or the Galerkin-Bubnov method. Because of the inherent difficulty in solving non-linear boundary-value problems, all the published work on shell stability from the large deflection point of view has been limited to the previously mentioned types of loading, which made the above simplification possible.

In this study, three types of loading conditions are considered; namely: radial pressure, live load (a vertical load distributed over the horizontal projection of the shell), and dead load (a vertical load distributed over the surface of the shell). It is noted that the latter two types of loading have a component in the circumferential direction, so that the simplification mentioned above is not applicable. Consequently the problem is treated in terms of all three displacement components u, v and w, and is solved approximately by the Rayleigh-Ritz method. In applying this method, w is chosen to be a first harmonic approximation of the shell deflection, while u and v are chosen not only to be the particular integrals (u_p, v_p) of the equilibrium equations (as was done in Ref. 9) but to contain also homogeneous solutions (u_h, v_h) so that the sums $u = u_p + u_h$, $v = v_p + v_h$ approximately satisfy the geometric and natural boundary conditions. The approximations involved are twofold. First, in considering the natural boundary conditions only the membrane forces N_x and N_ϕ are taken into account. (For "long" shells, these are the dominant forces.) Second, certain trigonometric functions describing the force distribution along the boundary are approximated by polynomials. Such approximations are necessary because it seems impossible to find a set of u and v so that the governing differential equations and all the associated boundary conditions are simultaneously and rigorously satisfied. With u and v chosen as described, even with only two undetermined parameters in the assumed radial deflection function w, physically meaningful results are obtained. These results depict the non-linear behavior of the shells considered.

This thesis also deals with shells supported by flexible, rectangular edge beams, which represent more realistic boundary conditions for concrete roof shells than that assumed by other researchers.

Briefly, the contents of this study are arranged as follows:

Chapter II gives an outline of the basic assumptions, as well as an expression of the total potential energy of the shell and the edge beams. A detailed discussion of the choice of the approximate deflection functions is also presented. The latter portion of the chapter describes the numerical solution of the non-linear equations resulting from an application of the Rayleigh-Ritz procedure.

The numerical results obtained in this investigation are presented in Chapter III, in which the influences of the types of loading and the properties of the shell on its behavior are considered. Then,the accuracy of the analysis is evaluated by comparing the solutions with a linear problem solved in the ASCE Manual No. 31 (1) (1952) and with a non-linear problem investigated by Kornishin and Mushtari (11), (1959).

In Chapter IV, in addition to a short summary of the work, some remarks are made concerning the relation of this study to the present practice of stability consideration in concrete roof shell design. Finally, some suggestions are offered for possible future work.

1.2. Review of Literature

In 1934, Donnell, (4) (1934) making use of von Kármán's (22) (1910) approach to the problem of large deflections of plates, formulated the non-linear governing differential equations for cylindrical shells by including in the strain tensor the quadratic terms in $\frac{\partial w}{\partial x}$ and $\frac{\partial w}{R\partial \phi}$. Later, von Kármán and Tsien (9), (1941) used the same formulation to investigate the buckling problem of cylinders under axial compression with the Rayleigh-Ritz procedure. In this celebrated work, stable post-buckling equilibrium configurations were found, corresponding to axial loads as low as 25% of the critical loads predicted by the classical small deflection theory. These important results partly explained the large discrepancies which existed between experimental and earlier theoretical results, and demonstrated dramatically the inadequacy of the classical small deflection theory in predicting the buckling load of thin shells.

Since that time, research efforts devoted to the investigation of the stability problem of shells have been very intense. The emphasis, however, has been restricted to axially symmetric, closed shells, such as complete circular cylinders, truncated conical shells and spherical shells. Very little work has been done on open shell panels, such as circular cylindrical roof panels of rectangular planform.

In the American Society of Civil Engineers Manual No. 31 (1), (1952), it is suggested that the buckling stress of a long circular cylindrical roof shell could be approximated by the critical stress of a long cylinder under axial compression obtained by Timoshenko (21), (1936), using the classical small deflection theory. But Karakas and Scalzi (8), (1961), who test-loaded a cylindrical shell panel made of reinforced plastic, showed that such an approximation oversimplifies the problem and leads to erroneous and even unsafe design. The shell was found to buckle at 32% of the critical stress calculated according to the suggestions of the ASCE Manual No. 31.

Koiter (10), (1956) investigated the postbuckling behavior of a narrow cylindrical panel, such as that occurring in stiffened cylindrical shells under axial compression. He conjectured that the behavior of a very narrow curved panel in the advanced postbuckling stage would approach the behavior of a flat plate panel of the same width.

Soderquist (18), (1960) investigated experimentally the buckling strength of a series of curved panels with rectangular stiffeners. The load was applied in compression axially, and measurements were made of the initial buckling stress. The ultimate strength of the panels was found to increase markedly with curvature, and the rate of increase to depend on the ratio of stiffener spacing to shell thickness.

Finkel'shtein (5), (1956) studied the buckling problem of a cylindrical panel under the combined action of axial compression and uniform transverse radial pressure. Considering the panel to be simply supported along the edges of the shell, he assumed that no moment would appear in the shell so long as the loads were below their critical buckling value. However, when buckling took place, large deformations were produced. Thus, the problem was reduced to a system of two non-linear differential equations. The unknown functions were the radial displacement w and the stress function ψ. The radial displacement was assumed to be the same as in the case of small displacements and was substituted into one of the differential equations which was solved for ψ. Substituting both w and ψ into the second equation, the author obtained a function Φ which contained the maximum deflection and the loading as its arguments. The function Φ was expressed as a Fourier series and, by equating its coefficients to zero, the conditions of buckling were obtained.

Kornishin and Mushtari (11), (1959) presented an algorithm applicable to the solution of nonlinear problems of the theory of shallow shells. They applied the algorithm to the buckling problem of a circular cylindrical panel of rectangular planform supported by "rollers" on all sides and loaded transversely by a uniform radial pressure. (At a roller support, w = 0, and the forces vanish.) As mentioned earlier, the simplicity of loading enabled them to express the problem in the form of an equilibrium equation in the radial direction and a strain compatibility equation in terms of a stress function, ψ , and w. They were both non-linear 4th order partial differential equations. After choosing a set of appropriate trigonometric functions containing a total of six arbitrary undetermined parameters for w and ψ , the differential equations were solved approximately using the Bubnov-Galerkin method. In this way the problem was reduced to a set of 6 cubic algebraic equations to be solved simultaneously. The authors then proposed an algorithm to solve approximately these non-linear algebraic equations. The results were presented in the form of a set of load-deflection curves for different parameters.

Sunakawa and Uemura (20), (1960) solved a problem similar to that of Kornishin and Mushtari (11) except that the straight edges were assumed to be clamped while the curved edges were simply supported. Using techniques similar to those employed by Kornishin and Mushtari, Sunakawa and Uemura approximated w and ψ by a polynominal containing only one arbitrary undetermined parameter.

The numerical results of the last two references, (11) and (20) will be further referred to in the later chapters of this thesis.

This brief review has included materials on the large deflection or buckling of cylindrical panels only, as they are of primary concern in the present study. A more comprehensive survey of published literature on the general theory of elastic stability of closed shells may be found in reviews by Langhaar (12), (1958), Nash (16), (1960) and Fung and Sechler (6), (1960).

1.3. Notation

The symbols used in this study are defined as they first appear in the text. They are summarized here in alphabetical order for convenient reference:

A = cross sectional area of edge beam;

A_i; B_j = coefficients relating to u_p, v_p, defined by Eqs. (2.21a-e) and (2.22a-h). i varies from 1 to 7, and j from 2 to 11;

a, b = depth and width of edge beams;

c_{ij}, d_{ij} = coefficients of Eq. (2.49a-b) as listed in Appendix II i and j vary from 1 to 3;

D = $\dfrac{Et^3}{12(1-\nu^2)}$ = flexural rigidity;

$(\ )_e$ = quantity to be evaluated at the junction of the edge beam and the shell;

E = Young's Modulus;

g, h	=	undetermined parameters defining the center deflection of edge beam and shell and the center deflection of shell, respectively;
G, H	=	$\frac{g}{t}$, $\frac{h}{t}$, respectively;
H_o	=	horizontal centroidal axis of edge beam;
I_H	=	moment of inertia of the beam section about the horizontal principal axis, H_o;
$J(X_n)$	=	Jacobian matrix of a system of equations evaluated at X_n;
K	=	$\frac{Et}{1-\nu^2}$ = extensional rigidity;
k_{ij}	=	coefficients of Eq. (2.50), defining the total potential of the shell system;
L	=	longitudinal length of shell;
M_ϕ, M_x	=	bending moments per unit of longitudinal and circumferential length, respectively;
$M_{x\phi}$, $M_{\phi x}$	=	circumferential and longitudinal twisting moments per unit of circumferential and longitudinal length, respectively;
N_x, N_ϕ	=	longitudinal and circumferential normal forces per unit of circumferential and longitudinal length, respectively;
$N_{x\phi}$, $N_{\phi x}$	=	circumferential and longitudinal shearing forces per unit of circumferential and longitudinal length, respectively;

$(\quad)^m_n$ = the superscript m indicates the number of the load increment applied, and the subscript n indicates the number of iterations performed by the computer;

P_x, P_ϕ, P_r = Intensities of load components in the longitudinal, circumferential, and radial directions, respectively. Their positive senses are orientated in the directions of positive x, y and z;

p_{RL} = intensity of radial load;

p_{LL} = intensity of live load;

p_{DL} = intensity of dead load;

$$\left.\begin{aligned} Q_x &= \frac{P_x}{E} \\ Q_\phi &= \frac{P_\phi}{E} \\ Q_r &= \frac{P_r}{E} \end{aligned}\right\}$$ = dimensionless load parameter in longitudinal, circumferential, and radial direction, respectively;

$$\left.\begin{aligned} q_{RL} &= \frac{p_{RL}}{E} \\ q_{LL} &= \frac{p_{LL}}{E} \\ q_{DL} &= \frac{p_{DL}}{E} \end{aligned}\right\}$$ = dimensionless load parameter of radial, live and dead load, respectively;

R = radius of shell;

s = curved length of shell;

S = $\frac{R}{L}$, dimensionless parameter of shell;

S_x, S_ϕ = transverse shearing forces per unit of circumferential and longitudinal length, respectively;

T	=	lateral thrust acting on the shell edge;
t	=	thickness of shell;
U	=	total potential energy of the shell system;
$\bar{U}$	=	$\frac{2Z}{EtR\phi_k L} U$
u, v, w	=	displacement components in the longitudinal, circumferential and radial direction, respectively;
$\bar{u} = \frac{u}{t}$, $\bar{v} = \frac{v}{t}$, $\bar{w} = \frac{w}{t}$	=	dimensionless displacement components in the longitudinal, circumferential and radial directions;
$\bar{u}_h, \bar{v}_h$	=	dimensionless displacement functions that satisfy the biharmonic equations of $\bar{u}$ and $\bar{v}$ respectively;
$\bar{u}_p, \bar{v}_p$	=	dimensionless displacement functions that satisfy the equilibrium equations in the axial direction, and the circumferential direction, respectively;
$\bar{u}_s, \bar{u}_B$	=	longitudinal displacement of the shell at $\eta = \pm 1/2$, and of the edge beam, respectively;
V	=	$\frac{a}{t}$, dimensionless shell parameter;
V_b	=	strain energy of edge beams;
V_s	=	strain energy of shell;
V_o	=	vertical centroidal axis of edge beam;
W	=	$\frac{b}{R}$, dimensionless shell parameter;
x, y, z	=	shell coordinates defining the mid-surface of the shell;

Z = $\frac{R}{t}$, dimensionless shell parameter;

α = horizontal displacement component of the edge beams along the centroidal axis H_o, positive to the right;

β = vertical displacement component of the edge beams along the centroidal axis V_o, positive upward;

$\bar{\beta}_S$, $\bar{\beta}_B$ = vertical displacement of the shell at $\eta = \pm\frac{1}{2}$, and of the edge beam, respectively;

ϵ_o = axial strain of the edge beam;

ϵ_x, ϵ_ϕ, $\epsilon_{x\phi}$ = longitudinal, circumferential and shear strain at the middle surface of shell, respectively;

$\left.\begin{matrix}\{\ \}_{\xi=\pm\frac{1}{2}} \\ \{\ \}_{\eta=\pm\frac{1}{2}}\end{matrix}\right\}$ = quantity is to be evaluated at $\xi = \pm\frac{1}{2}$, and $\eta = \pm\frac{1}{2}$, respectively;

ξ, η = dimensionless coordinates on middle surface;

θ_o = $\frac{\phi k}{2}$, rise angle of shell;

ν = Poisson's Ratio;

Ω = potential energy of the loads;

ϕ = shell coordinate in the circumferential direction;

ϕ_k = opening angle of shell;

λ_x, λ_ϕ, $\lambda_{x\phi}$ = longitudinal, circumferential curvature change, and twist of the middle surface, respectively;

Ψ = Airy Stress Function;

$$(\ )_{,x} = \frac{\partial(\ )}{\partial x}$$

$$\nabla^4 = (\quad)_{,xxxx} + \frac{2}{R^2}(\quad)_{,xx\phi\phi} + \frac{1}{R^4}(\quad)_{,\phi\phi\phi\phi}$$

$$\bar{\nabla}^4 = (\quad)_{,\xi\xi\xi\xi} + \frac{2}{\phi_k^2 S^2}(\quad)_{,\xi\xi\eta\eta} + \frac{1}{\phi_k^4 S^4}(\quad)_{,\eta\eta\eta\eta}$$

II. METHOD OF ANALYSIS

2.1. Shell Structure Considered

The shells considered in this investigation are shown in Fig. 2.1 and Fig. 2.2. The shell, with its mid-surface defined by the coordinates x and ϕ, is cut from a perfect circular cylindrical shell of constant thickness by two pairs of planes containing the principle radii of curvature. Fig. 2.1a depicts a shell supported by two identical rectangular flexible beams along the longitudinal edges and by rollers along the curved edges. The shell shown in Fig. 2.2 is supported by rollers along all edges.

The cross-section of the edge beams is shown in Fig. 2.1c in which V_o and H_o denote the vertical and horizontal centroidal axes, and β and α the corresponding displacements.

The external load applied on the shell is to be represented by the three components: P_x, P_ϕ, and P_r, denoting load intensities in the longitudinal, circumferential, and radial directions, respectively. The loading types considered are, as mentioned in Chapter I, radial load, live load, and dead load.

As usual, the symbols N_x, N_ϕ, $N_{x\phi}$, $N_{\phi x}$ denote the normal and shearing membrane forces; M_x, M_ϕ, $M_{x\phi}$, $M_{\phi x}$ are the bending and twisting moments; and S_x and S_ϕ are the transverse shearing forces acting on the shell. The positive directions of these internal forces are indicated in Fig. 2.1b.

2.2. Assumptions and Limitations

The analysis is based on a large deflection theory first advocated by Donnell (4), (1941). Associated with this theory are the following basic assumptions:

(1) The problem is restricted to small strains, i.e., the strains are small in comparison with unity.

(2) The problem is restricted to geometrical non-linearity. The material which forms the shell, however, remains linearly elastic so that Hooke's Law for a homogeneous and isotropic material may be applied.

(3) The shell under investigation is assumed to be thin; that is, $\frac{t}{R} \simeq \epsilon$ in which t and R are the thickness and radius of the shell, respectively, and ϵ is the strain in the x or ϕ direction. This assumption reduces the shell to a two dimensional problem and justifies the use of a simplified expression for strain energy of the shell by neglecting quantities having the same order of magnitude as $\frac{t}{R}$ in comparison with unity. It becomes possible to apply the Kirchhoff-Love hypothesis that vectors perpendicular to the mid-surface of the

shell before bending remain perpendicular after bending. At the same time normal stresses perpendicular to the mid-surface are considered to be small in comparison with the stresses tangential to the mid-surface. This hypothesis leads to an error of at most $\frac{t}{R}$ in comparison with unity. (17).

(4) In addition, the shell is assumed to be limited to "medium bending," that is, the maximum deflection is of the same order of magnitude as that of the thickness, but is small in comparison with other linear dimensions.

(5) The shell is also assumed to be shallow; that is, $\left(\frac{\phi_k}{2}\right)^2 = \left(\frac{s}{2R}\right)^2 << 1$ in which s is the curved length of the shell and ϕ_k is the opening angle. Except for one case, the maximum value of ϕ_k considered in this study is limited to $\phi_k = 0.632$ (approximately 36°) so that $\left(\frac{\phi_k}{2}\right)^2 \leq 0.1$.

(6) Furthermore, the shell considered is assumed to be long, i.e.,

$$\frac{\phi_k R}{L} \leq 0.5$$

in which L = longitudinal length of shell. In this way, the deformed shape of the shell might be closely approximated by a half cosine wave in both the longitudinal and circumferential directions, and the dominant internal forces will be the normal membrane forces N_x and N_ϕ.

The first five assumptions are generally made in most of the research work in the large deflection theory of shells. The additional sixth assumption is made to facilitate the development of the analytical procedure used in this study. Generally, these assumptions are applicable to reinforced concrete roof shells provided the opening angle is not too large.

2. 3. Potential Energy of the Shell System

As mentioned earlier, the method of Rayleigh-Ritz is used in this study. It is therefore necessary to have the expression of the potential energy of the shell system.

2. 3. 1. Strain-Displacement Relations of the Shell: Based upon assumptions outlined in section 2. 2., the strain of the mid-surface of the shell can be related to displacements u, v and w by the following expressions:

$$
\begin{aligned}
\epsilon_x &= u_{,x} + \frac{1}{2}(w_{,x})^2 \\
\epsilon_\phi &= \frac{1}{R}v_{,\phi} + \frac{w}{R} + \frac{1}{2R^2}(w_{,\phi})^2 \\
2\epsilon_{x\phi} &= v_{,x} + \frac{1}{R}u_{,\phi} + \frac{1}{R}w_{,x}\,w_{,\phi} \\
\lambda_x &= -w_{,xx} \\
\lambda_\phi &= -\frac{1}{R^2}w_{,\phi\phi} \\
\lambda_{x\phi} &= -\frac{1}{R}w_{,x\phi}
\end{aligned}
\qquad (2.1a\text{-}f)
$$

in which $\epsilon_x, \epsilon_\phi, \epsilon_{x\phi}$ = longitudinal, circumferential and shear strain in mid-surface, respectively.

$\chi_x, \chi_\phi, \chi_{x\phi}$ = longitudinal, circumferential curvature change, and twist of mid-surface, respectively.

The notation has been adopted that a comma followed by a subscript indicates a partial derivative. Thus $u_{,x} = \frac{\partial u}{\partial x}$ etc.

2.3.2. Strain Energy of Shell: The strain energy of the shell, V_s, can be expressed in the following form if quantities of the order of magnitude of $\frac{t}{R}$ in comparison with unity are neglected (13), (1962).

$$V_s = \frac{1}{2}\int_{-\frac{L}{2}}^{\frac{L}{2}}\int_{-\frac{\phi_k}{2}}^{\frac{\phi_k}{2}} \Big\langle K\left\{(\epsilon_x+\epsilon_\phi)^2 - 2(1-\nu)(\epsilon_x\epsilon_\phi - \epsilon_{x\phi}^2)\right\} + D\left\{(\chi_x+\chi_\phi)^2 - 2(1-\nu)(\chi_x\chi_\phi - \chi_{x\phi}^2)\right\}\Big\rangle R\,d\phi\,dx \qquad (2.2.)$$

in which

K = extensional rigidity $= \frac{Et}{(1-\nu^2)}$

D = flexural rigidity $= \frac{Et^3}{12(1-\nu^2)}$

ν = Poisson's ratio

E = Young's modulus

If the strain-displacement relations Eqs. (2.1a-f) are substituted into the strain energy expression of the shell, Eq. (2.2) becomes

$$V_s = \frac{1}{2}\int_{-\frac{L}{2}}^{\frac{L}{2}}\int_{-\frac{\phi_k}{2}}^{\frac{\phi_k}{2}} \Big\langle K\Big\{\Big[u_{,x}+\frac{1}{2}(w_{,x})^2+\frac{1}{R}v_{,\phi}+\frac{w}{R}+\frac{1}{2R^2}(w_{,\phi})^2\Big]^2-$$
$$-2(1-\nu)\Big\{\Big[u_{,x}+\frac{1}{2}(w_{,x})^2\Big]\Big[\frac{1}{R}v_{,\phi}+\frac{w}{R}+\frac{1}{2R^2}(w_{,\phi})^2\Big]-$$
$$-\frac{1}{4}\Big[v_{,x}+\frac{1}{R}u_{,\phi}+\frac{1}{R}w_{,x}w_{,\phi}\Big]^2\Big\}\Big\}+ \qquad (2.3.)$$
$$+D\Big\{\Big[w_{,xx}+\frac{1}{R^2}w_{,\phi\phi}\Big]^2-$$
$$-2(1-\nu)\Big[\frac{1}{R^2}w_{,xx}w_{,\phi\phi}-\frac{1}{R^2}(w_{,x\phi})^2\Big]\Big\}\Big\rangle R\,d\phi\,dx$$

2.3.3. Strain Energy of Edge Beam: Assuming that the displacements of the edge beams are small in comparison with their cross-sectional dimensions, the elementary beam theory will be used. Furthermore, in accordance with the accepted procedure of shell design (1), it is assumed that the edge beams have zero rigidity against bending in the horizontal plane and against twisting, and the strain energy due to shear deformation is negligible. Thus the strain energy of the two edge beams is:

$$V_b = \int_{-\frac{L}{2}}^{\frac{L}{2}}\Big\{EA(\epsilon_o)^2 + EI_H(\beta_{xx})^2\Big\}dx \qquad (2.4.)$$

A = (a)(b), a is the depth of the beams and b the width;

I_H $=\frac{a^3b}{12}$; moment of inertia of the beam cross section about the horizontal principal axis, H_o;

ϵ_o = axial strain of the edge beam.

The deformations of the edge beams are related to those of the shell by the following expressions:

$$\beta = w_e \cos\frac{\phi_k}{2} - v_e \sin\frac{\phi_k}{2}$$

$$\epsilon_o = (\epsilon_x)_e + \frac{a}{2}(\beta,_{xx})_e \tag{2.5.}$$

$$= (u,_x)_e + \frac{1}{2}(w,_x)_e^2 + \frac{a}{2}\left\{(w,_{xx})_e \cos\frac{\phi_k}{2} - (v,_{xx})_e \sin\frac{\phi_k}{2}\right\}$$

The subscript e indicates the quantity to be evaluated at the junction of the edge beam and the shell; i.e., at $\phi = \frac{\phi_k}{2}$

Substituting Eqs.(2.5) into Eq. (2.4) the total strain energy of the two edge beams becomes

$$V_b = \int_{-\frac{L}{2}}^{\frac{L}{2}} \left\langle EA\left\{(u,_x)_e + \frac{1}{2}(w,_x)_e^2 + \frac{a}{2}\left[(w,_{xx})_e \cos\frac{\phi_k}{2} - (v,_{xx})_e \sin\frac{\phi_k}{2}\right]\right\}^2 + \right.$$

$$\left. + EI_H\left\{\left[w_e \cos\frac{\phi_k}{2} - v_e \sin\frac{\phi_k}{2}\right],_{xx}\right\}^2 \right\rangle dx \tag{2.6.}$$

2.3.4. <u>Potential Energy of Loads on the Shell</u>: The potential energy of the loads acting on the shell domain is

$$\Omega = -\int_{-\frac{L}{2}}^{\frac{L}{2}}\int_{-\frac{\phi_k}{2}}^{\frac{\phi_k}{2}} (P_x u + P_\phi v + P_r w) R\,d\phi\,dx \tag{2.7.}$$

2.4. <u>Principle of Stationary Potential Energy of the Shell System</u>

The total potential energy of the shell system is:

$$U = V_s + V_b + \Omega \tag{2.8.}$$

in which V_s, V_b, and Ω are given by Eqs. (2.3), (2.6) and (2.7), respectively.

If the shell system is in equilibrium the variation of the total potential δU must vanish for any arbitrary virtual displacement, i.e.,

$$\delta U = \delta(V_s + V_b + \Omega) \equiv 0 \tag{2.9.}$$

2.5. Rayleigh-Ritz Method

Instead of solving the variational equation, Eq. (2.9), directly, the approximate method of Rayleigh-Ritz is applied. The procedure of solution is outlined as follows:

(1) A set of displacement functions, u, v, and w with n undetermined parameters are assumed and substituted into Eq. (2.8).

(2) The total potential of the shell system is made stationary with respect to the n undetermined parameters, i.e., the partial derivative of the total potential, U, with respect to each of the n parameters is obtained and set equal to zero.

(3) After carrying out the integration, the result is a set of n simultaneous non-linear algebraic equations from which the n parameters can be determined.

The above procedure yields the deflection of the shell for a given load intensity. By repeating this process for different values of the load, a load-deflection curve, which depicts the behavior of the shell, can be obtained.

2.6. Approach Used in Choosing Approximate Displacement Functions

2.6.1. General: The method of Rayleigh-Ritz has been successfully applied to stability problems of shell structures when the deflection functions chosen actually approximate the real deformed shapes of the shells observed in experiments. Such was the case of a circular cylinder in compression; the deflection functions used by various investigators approximated the diamond shape deflection pattern observed in laboratory tests. In the case of cylindrical panels under transverse loads, however, no definitive experimental data are available. However, one might suspect that the radial deflection w will be close to the first harmonic in both the longitudinal and circumferential directions. This approximation was found to be satisfactory by Kornishin and Mushtari (11), (1959) for cylindrical panels supported by rollers on all sides and loaded transversely by radial forces, provided that the assumptions listed in section 2.2 are satisfied. It is far more difficult, however, to estimate by physical intuition alone the forms of the displacement functions u and v. Chung and Veletsos (3), (1962), in solving the linear equilibrium problem of a cylindrical roof shell by means of the Rayleigh-Ritz method, used orthogonal trigonometric functions. By using all harmonics up to and including the 4th in each of the deflection functions, u, v, and w, they found the solutions converged to those given in ASCE Manual No. 31 (1). However, to investigate the non-linear behavior of the shell, these approximating functions with 15 arbitrary undetermined parameters may not be accurate enough as they do not satisfy the equilibrium equations of the shell in its interior, or the forced and natural boundary conditions.

In this investigation, the function w is chosen essentially on an intuitive basis and is limited to a first harmonic approximation. The functions, u and v, however, are not chosen arbitrarily. Rather, they are made consistent with the choice of w in that they satisfy exactly the equilibrium equations in the x and ϕ directions and approximately the associated boundary conditions. The displacement functions u and v may be considered to be composed of two parts:

$$u = u_p + u_h \qquad v = v_p + v_h \tag{2.10a-b}$$

in which u_p and v_p are the particular solutions of the equilibrium equations in the x and ϕ directions (Eqs. (2.11a-d), to be given later). In general, u_p and v_p do not satisfy all the natural and geometric boundary conditions. Therefore, the additional expressions, u_h and v_h, which are solutions of the homogeneous equilibrium equations, are obtained in such a manner that the sums $u_p + u_h$ and $v_p + v_h$ satisfy approximately the boundary conditions. In general, for each particular case of load type and boundary conditions, u and v must be derived individually.

2.6.2. <u>Equilibrium Equations of Shell</u>: The equilibrium equations for the x and ϕ directions of the shell can be obtained from a consideration of the equilibrium of a differential element of the shell (14), (1961). They are given as follows:

$$u_{,xx} + \left(\frac{1+\nu}{2}\right)\frac{1}{R}v_{,x\phi} + \left(\frac{1-\nu}{2}\right)\frac{1}{R}u_{,\phi\phi} + \frac{\nu}{R}w_{,x} + f_1 + \frac{P_x}{K} = 0$$

$$\frac{1}{R^2}v_{,\phi\phi} + \left(\frac{1+\nu}{2}\right)\frac{1}{R}u_{,x\phi} + \left(\frac{1-\nu}{2}\right)v_{,xx} + \frac{1}{R^2}w_{,\phi} + f_2 + \frac{P_\phi}{K} = 0 \qquad (2.11a\text{-}b)$$

in which

$$f_1 = \left[\frac{1}{2}(w_{,x})^2 + \frac{\nu}{2R^2}(w_{,\phi})^2\right]_{,x} + \left(\frac{1-\nu}{2}\right)\frac{1}{R^2}(w_{,x}w_{,\phi})_{,\phi}$$

$$f_2 = \frac{1}{R}\left[\frac{1}{2R^2}(w_{,\phi})^2 + \frac{\nu}{2}(w_{,x})^2\right]_{,\phi} + \left(\frac{1-\nu}{2}\right)\frac{1}{R}(w_{,x}w_{,\phi})_{,x} \qquad (2.11c\text{-}d)$$

Eqs. (2.11a-b) can be expressed in terms of w only by the use of the following relations:

$$\frac{2}{1-\nu}\frac{1}{R^2}\left\{Eq\,(2.11a)\right\}_{,\phi\phi} + \left\{Eq\,(2.11a)\right\}_{,xx} - \frac{1+\nu}{1-\nu}\frac{1}{R}\left\{Eq\,(2.11b)\right\}_{,x\phi} = 0 \qquad (2.12a\text{-}b)$$

$$\frac{1}{R^2}\left\{Eq\,(2.11b)\right\}_{,\phi\phi} + \frac{2}{1-\nu}\left\{Eq\,(2.11b)\right\}_{,xx} - \frac{1+\nu}{1-\nu}\frac{1}{R}\left\{Eq\,(2.11a)\right\}_{,x\phi} = 0$$

Then Eqs. (2.11a-b) are transformed into the following:

$$\nabla^4 u = -\frac{\nu}{R}w_{,xxx} + \frac{1}{R^3}w_{,x\phi\phi} - f_{1,xx} - \left(\frac{2}{1-\nu}\right)\frac{1}{R^2}f_{1,\phi\phi} + \left(\frac{1+\nu}{1-\nu}\right)\frac{1}{R}f_{2,x\phi} -$$

$$-\frac{1}{K}\left(\frac{2}{1-\nu}\right)\frac{1}{R^2}P_{x,\phi\phi} - \frac{1}{K}P_{x,xx} + \frac{1}{K}\left(\frac{1+\nu}{1-\nu}\right)\frac{1}{R}P_{\phi,x\phi}$$

$$(2.13a\text{-}b)$$

$$\nabla^4 v = -\frac{1}{R^4}w_{,\phi\phi\phi} - (2+\nu)\frac{1}{R^2}w_{,xx\phi} - \left(\frac{2}{1-\nu}\right)f_{2,xx} - \frac{1}{R^2}f_{2,\phi\phi} +$$

$$+\left(\frac{1+\nu}{1-\nu}\right)\frac{1}{R}f_{1,x\phi} - \frac{1}{KR^2}P_{\phi,\phi\phi} - \frac{1}{K}\left(\frac{2}{1-\nu}\right)P_{\phi,xx} + \frac{1}{K}\left(\frac{1+\nu}{1-\nu}\right)\frac{1}{R}P_{x,x\phi}$$

in which

$$\nabla^4 = (\quad)_{,xxxx} + \frac{2}{R^2}(\quad)_{,xx\phi\phi} + \frac{1}{R^4}(\quad)_{,\phi\phi\phi\phi}$$

Substituting the derivatives of f_1 and f_2 (Eqs. (2.11c-d)) into Eqs. (2.13a-b), then $\nabla^4 u$ and $\nabla^4 v$ become functions of w, the applied load, and their derivatives, as follows:

$$\begin{aligned}
\nabla^4 u = & -\frac{\nu}{R} w_{,xxx} + \frac{1}{R^3} w_{,x\phi\phi} - w_{,x} w_{,xxxx} - 3 w_{,xx} w_{,xxx} - \\
& - 2(2+\nu)\frac{1}{R^2} w_{,x\phi} w_{,xx\phi} - \frac{2}{R^2} w_{,x} w_{,xx\phi\phi} - \frac{(2-\nu)}{R^2} w_{,xx} w_{,x\phi\phi} - \\
& - \frac{1}{R^4} w_{,x} w_{,\phi\phi\phi\phi} - \frac{1}{R^4} w_{,\phi\phi} w_{,x\phi\phi} - \frac{2}{R^4} w_{,x\phi} w_{,\phi\phi\phi} + \\
& + \frac{\nu}{R^2} w_{,xxx} w_{,\phi\phi} - \frac{1}{KR^2}\left(\frac{2}{1-\nu}\right) P_{x,\phi\phi} - \frac{1}{K} P_{x,xx} + \frac{1}{KR}\left(\frac{1+\nu}{1-\nu}\right) P_{\phi,x\phi}
\end{aligned}$$

(2.14a-b)

$$\begin{aligned}
\nabla^4 v = & -\frac{1}{R^4} w_{,\phi\phi\phi} - \frac{2+\nu}{R^2} w_{,xx\phi} - \frac{2}{R^3} w_{,\phi} w_{,xx\phi\phi} - \frac{2(2+\nu)}{R^3} w_{,x\phi} w_{,x\phi\phi} - \\
& - \frac{(2-\nu)}{R^3} w_{,xx\phi} w_{,\phi\phi} - \frac{1}{R} w_{,\phi} w_{,xxxx} - \frac{1}{R} w_{,xx} w_{,xx\phi} - \\
& - \frac{2}{R} w_{,xxx} w_{,x\phi} - \frac{1}{R^5} w_{,\phi} w_{,\phi\phi\phi\phi} - \frac{3}{R^5} w_{,\phi\phi} w_{,\phi\phi\phi} + \\
& + \frac{\nu}{R^3} w_{,xx} w_{,\phi\phi\phi} - \frac{1}{KR^2} P_{\phi,\phi\phi} - \frac{1}{K}\left(\frac{2}{1-\nu}\right) P_{\phi,xx} + \\
& + \frac{1}{K}\left(\frac{1+\nu}{1-\nu}\right)\frac{1}{R} P_{x,x\phi}
\end{aligned}$$

2.6.3. Dimensionless Coordinates and Dimensionless Parameters:

In the following, the x and ϕ coordinates are expressed in terms of the dimensionless coordinate ξ and η ; in which

$$\xi = \frac{x}{L}$$

$$\eta = \frac{\phi}{\phi_k}$$

Furthermore, the properties of the shell system will be expressed in terms of ϕ_k, ν as well as the following dimensionless parameters:

$$S = \frac{R}{L}$$

$$Z = \frac{R}{t}$$

$$V = \frac{a}{t}$$

$$W = \frac{b}{R}$$

$$Q_x,\ Q_\phi,\ Q_r = \frac{P_x}{E},\ \frac{P_\phi}{E},\ \frac{P_r}{E},\ \text{respectively.}$$

At the same time, the displacements u, v, and w are expressed in the following dimensionless form:

$$\bar{u} = \frac{u}{t}$$

$$\bar{v} = \frac{v}{t}$$

$$\bar{w} = \frac{w}{t}$$

In terms of dimensionless coordinates and parameters and setting the Poisson ratio $\nu = 0$, the equilibrium equations, Eqs. (2.14a-b), are transformed into:

$$
\begin{aligned}
\overline{\nabla}^4 \bar{u} = {} & \frac{1}{S^3 \phi_K^2} \bar{w}_{,\xi\eta\eta} - \frac{S}{Z} \bar{w}_{,\xi} \bar{w}_{,\xi\xi\xi\xi} - \frac{3S}{Z} \bar{w}_{,\xi\xi} \bar{w}_{,\xi\xi\xi} - \\
& - \frac{4}{SZ\phi_K^2} \bar{w}_{,\xi\eta} \bar{w}_{,\xi\xi\eta} - \frac{2}{SZ\phi_K^2} \left(\bar{w}_{,\xi} \bar{w}_{,\xi\xi\eta\eta} + \bar{w}_{,\xi\xi} \bar{w}_{,\xi\eta\eta} \right) - \\
& - \frac{1}{S^3 Z \phi_K^4} \left(\bar{w}_{,\xi} \bar{w}_{,\eta\eta\eta\eta} + \bar{w}_{,\eta\eta} \bar{w}_{,\xi\eta\eta} + 2 \bar{w}_{,\xi\eta} \bar{w}_{,\eta\eta\eta} \right) - \\
& - \frac{2Z^2}{S^4 \phi_K^2} Q_{x,\eta\eta} - \frac{Z^2}{S^2} Q_{x,\xi\xi} + \frac{Z^2}{S^3 \phi_K} Q_{\phi,\xi\eta}
\end{aligned}
$$

(2.15a-b)

$$
\begin{aligned}
\overline{\nabla}^4 \bar{v} = {} & - \frac{1}{S^4 \phi_K^3} \bar{w}_{,\eta\eta\eta} - \frac{2}{S^2 \phi_K} \bar{w}_{,\xi\xi\eta} - \frac{2}{S^2 Z \phi_K^3} \bar{w}_{,\eta} \bar{w}_{,\xi\xi\eta\eta} - \\
& - \frac{1}{S^2 Z \phi_K^3} \left(4 \bar{w}_{,\xi\eta} \bar{w}_{,\xi\eta\eta} + 2 \bar{w}_{,\xi\xi\eta} \bar{w}_{,\eta\eta} \right) - \\
& - \frac{1}{Z \phi_K} \left(\bar{w}_{,\eta} \bar{w}_{,\xi\xi\xi\xi} + \bar{w}_{,\xi\xi} \bar{w}_{,\xi\xi\eta} + 2 \bar{w}_{,\xi\xi\xi} \bar{w}_{,\xi\eta} \right) - \\
& - \frac{1}{S^4 Z \phi_K^5} \left(\bar{w}_{,\eta} \bar{w}_{,\eta\eta\eta\eta} + 3 \bar{w}_{,\eta\eta} \bar{w}_{,\eta\eta\eta} \right) \\
& - \frac{Z^2}{S^4 \phi_K^2} Q_{\phi,\eta\eta} - \frac{2Z^2}{S^2} Q_{\phi,\xi\xi} + \frac{Z^2}{S^3 \phi_K} Q_{x,\xi\eta}
\end{aligned}
$$

in which

$$
\overline{\nabla}^4 = (\quad)_{,\xi\xi\xi\xi} + \frac{2}{\phi_K^2 S^2} (\quad)_{,\xi\xi\eta\eta} + \frac{1}{\phi_K^4 S^4} (\quad)_{,\eta\eta\eta\eta}
$$

2.7. Choice of $\bar{w}$

The displacement function w used in this investigation is given as follows:

$$w = g \cos\phi \cos\frac{\pi x}{L} + h \cos\frac{\pi\phi}{\phi_K} \cos\frac{\pi x}{L} \tag{2.16}$$

in which the parameter h accounts for part of the deflection at the center of the shell, while the other parameter g accounts for part of the deflection at the center of the shell and the deflection of the edge beams. Eq. (2.16) may be reduced to a dimensionless form as follows:

$$\bar{w} = G \cos\phi_K\eta \cos\pi\xi + H \cos\pi\eta \cos\pi\xi \tag{2.17}$$

in which

$$G = \frac{g}{t}$$

$$H = \frac{h}{t}$$

2.8. Choice of $\bar{u}_p$ and $\bar{v}_p$ to Satisfy Equilibrium Equations

2.8.1. Radial Load Case: For the case of a uniformly distributed radial load p_{RL}:

$$Q_x = 0$$

$$Q_\phi = 0 \tag{2.18a-c}$$

$$Q_r = \frac{p_{RL}}{E} = q_{RL}$$

Substituting Eqs. (2.17) and (2.18a-c) into Eqs. (2.15a-b), after several transformations, the following partial differential equations of $\bar{u}$ and $\bar{v}$ in terms of G and H are obtained.

$$
\begin{aligned}
\bar{\nabla}^4 \bar{u} = {} & G \frac{\pi}{s^3} \cos\phi_K\eta \sin\pi\xi + H \frac{\pi^3}{s^3 \phi_K^2} \cos\pi\eta \sin\pi\xi + (G^2 + H^2) \frac{2\pi^5 s}{z} \sin\pi\xi \cos\pi\xi + \\
& + GH \left\langle \left\{ 2\pi^2 + \frac{1}{s^2}\left[1 + \left(\frac{\pi}{\phi_K}\right)^2\right] \right\}^2 + 4\pi^4 \right\rangle \frac{\pi s}{z} \cos\phi_K\eta \cos\pi\eta \sin\pi\xi \cos\pi\xi - \\
& - GH \left\langle 4\pi^2 + \frac{1}{s^2}\left[1 + \left(\frac{\pi}{\phi_K}\right)^2\right] \right\rangle \frac{2\pi^2}{\phi_K s z} \sin\phi_K\eta \sin\pi\eta \sin\pi\xi \cos\pi\xi + \\
& + G^2 \left\langle \frac{2\pi s}{z} \left(\pi^2 + \frac{1}{s^2}\right)^2 \right\rangle \cos 2\phi_K\eta \sin\pi\xi \cos\pi\xi + \\
& + H^2 \left\langle \frac{2\pi^5 s}{z} \left(1 + \frac{1}{s^2 \phi_K^2}\right)^2 \right\rangle \cos 2\pi\eta \sin\pi\xi \cos\pi\xi
\end{aligned}
$$

(2.19a-b)

$$
\begin{aligned}
\bar{\nabla}^4 \bar{v} = {} & - G\left(\frac{1}{s^4} - \frac{2\pi^2}{s^2}\right) \sin\phi_K\eta \cos\pi\xi - H\left(\frac{\pi^3}{\phi_K^3 s^4} + \frac{2\pi^3}{\phi_K s^2}\right) \sin\pi\eta \cos\pi\xi + \\
& + G^2 \frac{2}{s^4 z} \sin\phi_K\eta \cos\phi_K\eta + GH \left[1 + 3\left(\frac{\pi}{\phi_K}\right)^2\right] \frac{\pi}{2\phi_K s^4 z} \cos\phi_K\eta \sin\pi\eta + \\
& + GH \left[3 + \left(\frac{\pi}{\phi_K}\right)^2\right] \frac{\pi^2}{2\phi_K^2 s^4 z} \sin\phi_K\eta \cos\pi\eta + H^2 \frac{2\pi^5}{\phi_K^5 s^4 z} \sin\pi\eta \cos\pi\eta + \\
& + G^2 \left[\pi^2 + \frac{1}{s^2}\right]^2 \left(\frac{2}{z}\right) \sin\phi_K\eta \cos\phi_K\eta \cos 2\pi\xi + \\
& + GH \left\{ \left[2\pi^2 + \frac{1}{s^2}\right]^2 + \frac{4\pi^2}{s^2} + \frac{3\pi^2}{\phi_K^2 s^4} \right\} \frac{\pi}{2\phi_K z} \cos\phi_K\eta \sin\pi\eta \cos 2\pi\xi + \\
& + GH \left\{ \pi^2 \left[2\phi_K^2 + \frac{1}{s^2}\right]^2 + \frac{4\pi^2}{s^2} + \frac{3}{s^4} \right\} \frac{\pi^2}{2\phi_K^2 z} \sin\phi_K\eta \cos\pi\eta \cos 2\pi\xi + \\
& + H^2 \left[1 + \frac{1}{\phi_K^2 s^2}\right]^2 \frac{2\pi^5}{\phi_K z} \sin\pi\eta \cos\pi\eta \cos 2\pi\xi
\end{aligned}
$$

It is noted that Eqs. (2.19a-b) do not involve any loading term because the consideration of equilibrium condition in x and ϕ directions does not involve the radial load. Thus, a particular solution of Eqs. (2.19a-b) is found to be the following:

$$\bar{u}_p = G A_1 \cos\phi_K\eta \sin\pi\xi + H A_2 \cos\pi\eta \sin\pi\xi + (G^2 + H^2) A_3 \sin\pi\xi \cos\pi\xi +$$

$$+ G^2 A_4 \cos 2\phi_K\eta \sin\pi\xi \cos\pi\xi + GH A_5 \cos\phi_K\eta \cos\pi\eta \sin\pi\xi \cos\pi\xi +$$

$$+ GH A_6 \sin\phi_K\eta \sin\pi\eta \sin\pi\xi \cos\pi\xi + H^2 A_7 \cos 2\pi\eta \sin\pi\xi \cos\pi\xi$$

(2.20a-b)

$$\bar{v}_p = G B_2 \sin\phi_K\eta \cos\pi\xi + H B_3 \sin\pi\eta \cos\pi\xi +$$

$$+ G^2 B_4 \sin\phi_K\eta \cos\phi_K\eta + GH B_5 \cos\phi_K\eta \sin\pi\eta +$$

$$+ GH B_6 \sin\phi_K\eta \cos\pi\eta + H^2 B_7 \sin\pi\eta \cos\pi\eta +$$

$$+ G^2 B_8 \sin\phi_K\eta \cos\phi_K\eta \cos 2\pi\xi + GH B_9 \cos\phi_K\eta \sin\pi\eta \cos 2\pi\xi +$$

$$+ GH B_{10} \sin\phi_K\eta \cos\pi\eta \cos 2\pi\xi + H^2 B_{11} \sin\pi\eta \cos\pi\eta \cos 2\pi\xi$$

in which

$$A_1 = \frac{\pi s}{(1+\pi^2 s^2)^2}$$

$$A_2 = \frac{\phi_K^2 s}{\pi(1+\phi_K^2 s^2)^2}$$

$$A_3 = A_4 = A_7 = \frac{\pi\phi_K s}{8} \qquad (2.21a\text{-}e)$$

$$A_5 = \frac{a_1 a_2 - a_3 a_4}{a_2^2 - a_4^2}$$

$$A_6 = \frac{a_1 a_4 - a_3 a_2}{a_2^2 - a_4^2}$$

$$
\begin{aligned}
a_1 &= \left[(2\pi^2\phi_K^2 s^2 + \phi_K^2 + \pi^2)^2 + 4\pi^4\phi_K^4 s^4\right] \pi\phi_K s \\
a_2 &= (4\pi^2\phi_K^2 s^2 + \pi^2 + \phi_K^2)^2 + 4\pi^2\phi_K^2 \\
a_3 &= (4\pi^2\phi_K^2 s^2 + \pi^2 + \phi_K^2)\, 2\pi^2\phi_K^2 s \\
a_4 &= (4\pi^2\phi_K^2 s^2 + \pi^2 + \phi_K^2)\, 4\pi\phi_K
\end{aligned}
$$

$$
\begin{aligned}
B_2 &= -\frac{(1+2\pi^2 s^2)}{(\pi^2 s^2 + 1)^2} \\
B_3 &= -\frac{\phi_K(1+2\phi_K^2 s^2)}{\pi(1+\phi_K^2 s^2)^2} \\
B_4 &= B_8 = \frac{\phi_K}{8} \\
B_5 &= \frac{b_1 b_2 - b_3 b_4}{b_2^2 - b_4^2} \\
B_6 &= \frac{b_3 b_2 - b_1 b_4}{b_2^2 - b_4^2} \\
B_7 &= B_{11} = \frac{\pi}{8} \\
B_9 &= \frac{b_5 b_6 - b_7 b_8}{b_6^2 - b_8^2} \\
B_{10} &= \frac{b_7 b_6 - b_5 b_8}{b_6^2 - b_8^2}
\end{aligned}
\qquad (2.22\text{a-h})
$$

$$
\begin{aligned}
b_1 &= (\phi_K^2 + 3\pi^2)\frac{\pi\phi_K^2}{2} \quad ; \quad b_2 = \left[(\pi^2 + \phi_K^2)^2 + 4\pi^2\phi_K^2\right] \\
b_3 &= (\pi^2 + 3\phi_K^2)\frac{\pi^2\phi_K}{2} \quad ; \quad b_4 = 4\pi\phi_K(\pi^2 + \phi_K^2) \\
b_5 &= \left[\phi_K^2(2\pi^2 s^2 + 1)^2 + 4\pi^2\phi_K^2 s^2 + 3\pi^2\right]\frac{\pi\phi_K^2}{2} \\
b_6 &= a_2 \quad ; \quad b_8 = a_4 \\
b_7 &= \left[\pi^2(2\phi_K^2 s^2 + 1)^2 + 4\pi^2\phi_K^2 s^2 + 3\phi_K^2\right]\frac{\pi^2\phi_K}{2}
\end{aligned}
$$

2.8.2. Live Load Case: For the shell system subjected to a uniform vertical live load p_{LL}, the force components can be expressed in terms of p_{LL} as follows:

$$
\begin{aligned}
Q_x &= 0 \\
Q_\phi &= \frac{p_{LL}}{E}\sin\phi\cos\phi = q_{LL}\sin\phi_k\eta\cos\phi_k\eta \qquad (2.23a\text{-}c)\\
Q_r &= \frac{p_{LL}}{E}\cos^2\phi = q_{LL}\cos^2\phi_k\eta
\end{aligned}
$$

If Eqs. (2.17) and (2.23a-c) are substituted into Eqs. (2.15a-b), the following equations are obtained:

$$
\begin{aligned}
\overline{\nabla}^4\bar{u} &= \text{Right hand side of Eq. (2.19a)} \qquad (2.24a\text{-}b)\\
\overline{\nabla}^4\bar{v} &= \text{Right hand side of Eq. (2.19b)} + q_{LL}\frac{2z^2}{S^4}\sin 2\phi_k\eta
\end{aligned}
$$

Then a particular solution of Eqs. (2.24a-b) for the uniform live load case is found to be

$$
\begin{aligned}
\bar{u}_p &= \text{Right hand side of Eq. (2.20a)} \qquad (2.25a\text{-}b)\\
\bar{v}_p &= \text{Right hand side of Eq. (2.20b)} + q_{LL}\frac{z^2}{8}\sin 2\phi_k\eta
\end{aligned}
$$

2.8.3. Dead Load Case: For a shell subjected to a uniform dead load p_{DL}, the force components can be expressed as follows:

$$
\begin{aligned}
Q_x &= 0 \\
Q_\phi &= \frac{p_{DL}}{E}\sin\phi = q_{DL}\sin\phi_k\eta \qquad (2.26a\text{-}c)\\
Q_r &= -\frac{p_{DL}}{E}\cos\phi = -q_{DL}\cos\phi_k\eta
\end{aligned}
$$

Substituting Eqs. (2.17) and (2.26a-c) into Eqs. (2.15a-b), the following equations are obtained:

$$
\begin{aligned}
\overline{\nabla}^4\bar{u} &= \text{Right hand side of Eq. (2.19a)} \qquad (2.27a\text{-}b)\\
\overline{\nabla}^4\bar{v} &= \text{Right hand side Eq. (2.19b)} + q_{DL}\frac{z^2}{S^4}\sin\phi_k\eta
\end{aligned}
$$

Then a particular solution of Eqs. (2.27a-b) for the dead load case is found to be:

$$\bar{u}_p = \text{Right hand side of Eq. (2.20a)} \qquad (2.28a\text{-}b)$$

$$\bar{v}_p = \text{Right hand side of Eq. (2.20b)} + q_{DL} z^2 \sin\phi_K \eta$$

2.9. Choice of $\bar{u}_h$ and $\bar{v}_h$ to Satisfy Boundary Conditions

2.9.1. General: It has been pointed out that the particular solutions of $\bar{u}_p$ and $\bar{v}_p$ given in Section 2.8 generally will not satisfy the geometric and natural boundary conditions of the shell. In passing, it may be mentioned that when $\bar{w}$, $\bar{u}_p$ and $\bar{v}_p$ alone are applied to the Rayleigh-Ritz procedure, the load-deflection response of the shell is very 'stiff' and exhibits only mild nonlinearity even at large deflections. If, however, the assumed functions of $\bar{u}_p$ and $\bar{v}_p$ are modified by $\bar{u}_h$ and $\bar{v}_h$ so that the geometric and the natural boundary conditions are approximately satisfied, the same shell shows a marked decrease of stiffness when the deflection becomes sufficiently large (See Fig. A.1 in Appendix I).

In the following, the procedure for obtaining $\bar{u}_h$ and $\bar{v}_h$ will be discussed in detail for shell systems

(a) with all edges supported on rollers, and

(b) with the longitudinal edges supported by flexible beams while the curved edges are supported by rollers.

2.9.2. Shells Supported by Rollers on All Sides: Along the curved edges, the boundary conditions corresponding to roller supports are expressed in dimensionless form as follows:

$$\{\bar{w}\}_{\xi=\pm\frac{1}{2}} = 0$$

$$\{\bar{M}_x\}_{\xi=\pm\frac{1}{2}} = -\frac{s^2}{12z^2}\{\bar{w}_{,\xi\xi}\}_{\xi=\pm\frac{1}{2}} = 0$$

$$\{\bar{N}_x\}_{\xi=\pm\frac{1}{2}} = \frac{s}{z}\left\{\bar{u}_{,\xi} + \frac{s}{2z}(\bar{w}_{,\xi})^2\right\}_{\xi=\pm\frac{1}{2}} = 0 \qquad (2.29\text{a-d})$$

$$\{\bar{N}_{x\phi}\}_{\xi=\pm\frac{1}{2}} = \frac{s}{2z}\left\{\bar{v}_{,\xi} + \frac{1}{\phi_k s}\bar{u}_{,\eta} + \frac{1}{\phi_k z}\bar{w}_{,\xi}\bar{w}_{,\eta}\right\}_{\xi=\pm\frac{1}{2}} = 0$$

in which $\{\ \}_{\xi=\pm\frac{1}{2}}$ indicates that the quantity is to be evaluated at $\xi=\pm\frac{1}{2}$. Along the longitudinal edges, the boundary conditions for roller support are as follows:

$$\{\bar{w}\}_{\eta=\pm\frac{1}{2}} = 0$$

$$\{\bar{M}_\phi\}_{\eta=\pm\frac{1}{2}} = -\frac{1}{12z^2\phi_k^2}\{\bar{w}_{,\eta\eta}\}_{\eta=\pm\frac{1}{2}} = 0 \qquad (2.30\text{a-d})$$

$$\{\bar{N}_\phi\}_{\eta=\pm\frac{1}{2}} = \frac{1}{z}\left\{\frac{1}{\phi_k}\bar{v}_{,\eta} + \bar{w} + \frac{1}{2z\phi_k^2}(\bar{w}_{,\eta})^2\right\}_{\eta=\pm\frac{1}{2}} = 0$$

$$\{\bar{N}_{\phi x}\}_{\eta=\pm\frac{1}{2}} = \frac{s}{2z}\left\{\bar{v}_{,\xi} + \frac{1}{\phi_k s}\bar{u}_{,\eta} + \frac{1}{\phi_k z}\bar{w}_{,\xi}\bar{w}_{,\eta}\right\}_{\eta=\pm\frac{1}{2}} = 0$$

In general, it seems impossible to find a $\bar{u}_h$ and $\bar{v}_h$ such that $\bar{u} = \bar{u}_p + \bar{u}_h$ and $\bar{v} = \bar{v}_p + \bar{v}_h$ satisfy exactly the boundary condition Eqs. (2.29a-d) and (2.30a-d) simultaneously. In the particular case of roller supports on all edges, G in Eqs. (2.17) and (2.20a-b) is set equal to zero. The resulting equations reduce to functions of H alone. When these simplified expressions for $\bar{w}$, $\bar{u}_p$, and $\bar{v}_p$ are substituted into the boundary condition equations, it is found that only Eqs. (2.29a-b) and (2.30a-b) are satisfied, while the membrane forces

$$\{\bar{N}_x\}_{\xi=\pm\frac{1}{2}}\ , \quad \{\bar{N}_{x\phi}\}_{\xi=\pm\frac{1}{2}}\ , \quad \{\bar{N}_{\phi x}\}_{\eta=\pm\frac{1}{2}},\ \text{and}\quad \{\bar{N}_\phi\}_{\eta=\pm\frac{1}{2}}$$

do not vanish on the boundary. The additional terms $\bar{u}_h$ and $\bar{v}_h$ are then chosen so that only Eqs. (2.29c) and (2.30c) are also satisfied; i.e., $\{\bar{N}_x\}_{\xi=\pm\frac{1}{2}} = 0$ and $\{\bar{N}_\phi\}_{\eta=\pm\frac{1}{2}} = 0$. A justification for this procedure may be, as indicated earlier, that the dominant internal forces for long shells ($\frac{R\phi_k}{L} < 0.5$) are N_x and N_ϕ. These forces probably contribute more to the non-linear behavior of shells than any other stress resultant (1).

2.9.2.a. <u>Radial Load Case</u>: For a shell supported by rollers on all edges, G = 0. Under the action of radial pressure, the deflection functions are reduced to the following:

$$\bar{w} = H \cos\pi\eta \cos\pi\xi \tag{2.31a-c}$$

$$\bar{u}_p = H A_2 \cos\pi\eta \sin\pi\xi + H^2(A_3 + A_7 \cos 2\pi\eta) \sin\pi\xi \cos\pi\xi$$

$$\bar{v}_p = H B_3 \sin\pi\eta \cos\pi\xi + H^2(B_7 + B_{11} \cos 2\pi\xi) \sin\pi\eta \cos\pi\eta$$

After substituting Eqs. (2.10a-b) into Eqs. (2.29c) and (2.30c), the following relations are obtained:

$$\{\bar{N}_x\}_{\xi=\pm\frac{1}{2}} = \frac{S}{Z}\left\{\bar{u}_{p,\xi} + \bar{u}_{h,\xi} + \frac{S}{2Z}(\bar{w}_{,\xi})^2\right\}_{\xi=\pm\frac{1}{2}} = 0 \tag{2.32a-b}$$

$$\{\bar{N}_\phi\}_{\eta=\pm\frac{1}{2}} = \frac{1}{Z}\left\{\frac{1}{\phi_k}\bar{v}_{p,\eta} + \frac{1}{\phi_k}\bar{v}_{h,\eta} + \bar{w} + \frac{1}{2Z\phi_k^2}(\bar{w}_{,\eta})^2\right\}_{\eta=\pm\frac{1}{2}} = 0$$

Eqs. (2.32a-b) imply that

$$\{\bar{u}_{h,\xi}\}_{\xi=\pm\frac{1}{2}} = -\{\bar{u}_{p,\xi} + \frac{\xi}{2z}(\bar{w}_{,\xi})^2\}_{\xi=\pm\frac{1}{2}}$$
$$\{\bar{v}_{h,\eta}\}_{\eta=\pm\frac{1}{2}} = -\{\bar{v}_{p,\eta} + \phi_K\bar{w} + \frac{1}{2z\phi_K}(\bar{w}_{,\eta})^2\}_{\eta=\pm\frac{1}{2}} \qquad (2.33a\text{-}b)$$

when substituting the values of $\bar{u}_p$, $\bar{v}_p$ and $\bar{w}_p$, taken from Eqs.(2.31a-c) into Eqs. (2.33a-b) the following relations are obtained:

$$\{\bar{u}_{h,\xi}\}_{\xi=\pm\frac{1}{2}} = H^2(\pi A_3 - \frac{5\pi^2}{4z})(1+\cos 2\pi\eta)$$
$$\{\bar{v}_{h,\eta}\}_{\eta=\pm\frac{1}{2}} = H^2(\pi B_7 - \frac{\pi^2}{4\phi_K z})(1+\cos 2\pi\xi) \qquad (2.34a\text{-}b)$$

Since $\bar{u}_h$ and $\bar{v}_h$ have to satisfy the biharmonic equations

$$\bar{\nabla}^4\bar{u}_h = 0 \; ; \qquad \bar{\nabla}^4\bar{v}_h = 0$$

the trigonometric expressions $(1+\cos 2\pi\eta)$ and $(1+\cos 2\pi\xi)$ are replaced by approximating polynomials $2(1-2\eta)$ and $2(1-2\xi)$, respectively, for all η defined in $0 \le \eta \le \frac{1}{2}$, and ξ defined in $0 \le \xi \le \frac{1}{2}$.
Then $\bar{u}_h$ and $\bar{v}_h$ may be written as the follwoing:

$$\bar{u}_h = H^2(2)(\pi A_3 - \frac{5\pi^2}{4z})\,\xi\,(1-2\eta)$$
$$\bar{v}_h = H^2(2)(\pi B_7 - \frac{\pi^2}{4\phi_K z})\,\eta\,(1-2\xi) \qquad (2.35a\text{-}b)$$

It is noted that the original trigonometric functions are even over the intervals $-\frac{1}{2} \le \xi \le \frac{1}{2}$; $-\frac{1}{2} \le \eta \le \frac{1}{2}$. Since the approximating polynomial expressions are defined only over the intervals $0 \le \xi \le \frac{1}{2}$, $0 \le \eta \le \frac{1}{2}$, the energy integrals, in changing to the approximating polynomials and the corresponding new limits of integration, must be multiplied by 2.

It should be pointed out also that the polynomials are close approximations of the trigonometric functions. Over the interval of definition, the polynomials have approximately the same shape as the trigonometric expressions; and in this particular case, have identical "area" under the curves. Since these expressions essentially represent the distribution of N_x and N_ϕ on the boundaries, the "same area" aspect implies that the replacement is "statically equivalent" to the original trigonometric functions. In short, this replacement of the trigonometric functions by the polynomials physically means that instead of N_x and N_ϕ strictly vanishing on the boundary, there will be a small residual distribution of these forces equal to the differences between the trigonometric and polynomial functions.

2.9.2.b. Live Load Case: In a procedure similar to that used in the radial load case, the deflection functions are found to be as follows:

$$
\begin{aligned}
\bar{w} &= \text{Right hand side of Eq. (2.31a)} \\
\bar{u}_p &= \text{Right hand side of Eq. (2.31b)} \\
\bar{v}_p &= \text{Right hand side of Eq. (2.31c)} + q_{LL}\frac{2z^2}{S^4}(\sin 2\phi_k \eta) \\
\bar{u}_h &= \text{Right hand side of Eq. (2.35a)} \\
\bar{v}_h &= \text{Right hand side of Eq. (2.35b)} - q_{LL}\frac{z^2\phi_k}{4}(\cos\phi_k)\eta
\end{aligned}
\qquad (2.36a\text{-}e)
$$

2.9.2.c. Dead Load Case: Similarly, in this case,

$$\begin{aligned}
\bar{w} &= \text{Right hand side of Eq. (2.31a)} \\
\bar{u}_p &= \text{Right hand side of Eq. (2.31b)} \\
\bar{v}_p &= \text{Right hand side of Eq. (2.31c)} + q_{DL} z^2 (\sin \phi_K \eta) \\
\bar{u}_h &= \text{Right hand side of Eq. (2.35a)} \\
\bar{v}_h &= \text{Right hand side of Eq. (2.35b)} - q_{DL} z^2 \phi_K \left(\cos \tfrac{\phi_K}{2}\right) \eta
\end{aligned} \qquad (2.37\text{a-e})$$

2.9.3. Shells Supported by Rollers on Curved Edges, and Rectangular Beams on the Longitudinal Edges:

Along the curved edges, the boundary conditions are given by Eqs. (2.29a-d). Along the longitudinal edges, however, if the edge beams are assumed to have zero rigidity against lateral bending and twisting as indicated in Section 2.3.3, the boundary conditions are as follows:

$$\begin{aligned}
\{T\}_{\eta=\pm\frac{1}{2}} &= 0 \\
\{M_\phi\}_{\eta=\pm\frac{1}{2}} &= 0 \\
\bar{u}_s &= \bar{u}_B \\
\bar{\beta}_s &= \bar{\beta}_B
\end{aligned} \qquad (2.38\text{a-d})$$

in which

$\{T\}_{\eta=\pm\frac{1}{2}}$ = lateral thrust acting on shell edge at $\eta = \pm\frac{1}{2}$;

$\bar{u}_s$, $\bar{u}_B$ = longitudinal displacement of shell at $\eta = \pm\frac{1}{2}$, and of the edge beam, respectively;

$\bar{\beta}_S, \bar{\beta}_B$ = vertical displacement of the shell at $\eta = \pm\frac{1}{2}$, and of the edge beam, respectively.

Eq. (2.38a) can be expressed in terms of the following boundary forces:

$$\{T\}_{\eta=\pm\frac{1}{2}} = \left\{\bar{N}_\phi \cos\frac{\phi_K}{2} + \bar{S}_\phi \sin\frac{\phi_K}{2}\right\}_{\eta=\pm\frac{1}{2}} \equiv 0 \qquad (2.39)$$

For thin and shallow shells, $\bar{N}_\phi \cos\frac{\phi_K}{2} \gg \bar{S}_\phi \sin\frac{\phi_K}{2}$.

Eq. (2.39) is then simplified to the following:

$$\{T\}_{\eta=\pm\frac{1}{2}} = \left\{\bar{N}_\phi \cos\frac{\phi_K}{2}\right\}_{\eta=\pm\frac{1}{2}} \equiv 0 \qquad (2.40)$$

In terms of dimensionless displacements:

$$\left\{\bar{N}_\phi \cos\frac{\phi_K}{2}\right\}_{\eta=\pm\frac{1}{2}} = \frac{1}{z}\cos\frac{\phi_K}{2}\left\{\frac{1}{\phi_K}\bar{v}_{,\eta} + \bar{w} + \frac{1}{2z\phi_K^2}(\bar{w}_{,\eta})^2\right\}_{\eta=\pm\frac{1}{2}} \equiv 0 \qquad (2.41)$$

2.9.3.a. <u>Dead Load Case</u>: For shells acted upon by dead load, the deflection functions $\bar{w}$, $\bar{u}_p$ and $\bar{v}_p$ expressed by Eqs. (2.17) and (2.28a-b), respectively, do not satisfy all the boundary condition equations (2.29a-d) and (2.38a-d). Again it will be impossible to find a $\bar{u}_h$ and a $\bar{v}_h$ so that all these boundary conditions are rigorously fulfilled simultaneously. However, it can be shown that Eqs.(2.17) and (2.28a-b) satisfy the boundary conditions Eqs.(2.29a-b) identically. In addition, $\bar{u}_h$ and $\bar{v}_h$ are chosen in such a way that Eqs. (2.29c) and (2.41) are satisfied; i.e.,

$$\{\bar{N}_x\}_{\xi=\pm\frac{1}{2}} = 0 \quad \text{and} \quad \left\{\bar{N}_\phi \cos\frac{\phi_K}{2}\right\}_{\eta=\pm\frac{1}{2}} = 0.$$

A possible justification of such a choice is similar to that stated in the previous section; that is, both $\{N_x\}_{\xi=\pm\frac{1}{2}}$ and $\{N_\phi \cos\frac{\phi_k}{2}\}_{\eta=\pm\frac{1}{2}}$ are the dominant boundary forces.

When Eqs. (2.10a-b) are substituted into Eqs. (2.29c) and (2.41), the following relations are obtained:

$$\{\bar{N}_x\}_{\xi=\pm\frac{1}{2}} = \frac{S}{Z}\left\{\bar{u}_{p,\xi} + \bar{u}_{h,\xi} + \frac{S}{2Z}(\bar{w}_{,\xi})^2\right\}_{\xi=\pm\frac{1}{2}} = 0$$
$$\{\bar{N}_\phi \cos\tfrac{\phi_k}{2}\}_{\eta=\pm\frac{1}{2}} = \frac{1}{Z}\cos\frac{\phi_k}{2}\left\{\frac{1}{\phi_k}\bar{v}_{p,\eta} + \frac{1}{\phi_k}\bar{v}_{h,\eta} + \bar{w} + \frac{1}{2Z\phi_k^2}(\bar{w}_{,\eta})^2\right\}_{\eta=\pm\frac{1}{2}} = 0 \qquad (2.42a\text{-}b)$$

Eqs. (2.42a-b) imply that

$$\{\bar{u}_{h,\xi}\}_{\xi=\pm\frac{1}{2}} = -\left\{\bar{u}_{p,\xi} + \frac{S}{2Z}(\bar{w}_{,\xi})^2\right\}_{\xi=\pm\frac{1}{2}}$$
$$\{\bar{v}_{h,\eta}\}_{\eta=\pm\frac{1}{2}} = -\left\{\bar{v}_{p,\eta} + \phi_k\bar{w} + \frac{1}{2Z\phi_k}(\bar{w}_{,\eta})^2\right\}_{\eta=\pm\frac{1}{2}} \qquad (2.43a\text{-}b)$$

Substituting the values of $\bar{w}$, $\bar{u}_p$, and $\bar{v}_p$ from Eqs. (2.17) and (2.28a-b) into Eqs. (2.43a-b), the following relations are obtained:

$$\{\bar{u}_{h,\xi}\}_{\xi=\pm\frac{1}{2}} = \Big\{G^2\left(\pi A_3 - \frac{\pi^2 S}{4Z}\right)(1+\cos 2\phi_k\eta) + GH\pi\left(A_5 - \frac{\pi S}{Z}\right)\cos\phi_k\eta\cos\pi\eta +$$
$$+ GH\pi A_6 \sin\phi_k\eta\sin\pi\eta + H^2\left(\pi A_3 - \frac{\pi^2 S}{4Z}\right)(1+\cos 2\pi\eta)\Big\}$$

(2.44a-b)

$$\{\bar{v}_{h,\eta}\}_{\eta=\pm\frac{1}{2}} = \Big\{-B_D\phi_k\cos\frac{\phi_k}{2} - G(\phi_k + B_2\phi_k)\cos\frac{\phi_k}{2}\cos\pi\xi -$$
$$- G^2\left[B_4\phi_k\left(\cos^2\frac{\phi_k}{2} - \sin^2\frac{\phi_k}{2}\right) + \frac{\phi_k}{4Z}\sin^2\frac{\phi_k}{2}\right](1+\cos 2\pi\xi) +$$
$$+ GH\Big[\left(\phi_k B_5 + \pi B_6 - \frac{\pi}{2Z}\right)\sin\frac{\phi_k}{2} +$$
$$+ \left(\phi_k B_9 + \pi B_{10} - \frac{\pi}{2Z}\right)\sin\frac{\phi_k}{2}\cos 2\pi\xi\Big] +$$
$$+ H^2\left[\pi B_7 - \frac{\pi^2}{4Z\phi_k}\right](1+\cos 2\pi\xi)\Big\}$$

in which $B_D = q_{DL} Z^2$

In order to have $\bar{u}_h$ and $\bar{v}_h$ satisfy the biharmonic equations, the trigonometric expressions in ξ and η are replaced by approximating polynomials as follows:

$$(1+\cos 2\phi_K\eta) \simeq 2-(1-\cos\phi_K)2\eta$$

$$(\cos\phi_K\eta \cos\pi\eta) \simeq 1-2\eta$$

$$(\sin\phi_K\eta \sin\pi\eta) \simeq 2\left(\sin\frac{\phi_K}{2}\right)\eta$$

$$(1+\cos 2\pi\eta) \simeq 2(1-2\eta)$$

for all values of η defined in the interval $0 \leq \eta \leq \frac{1}{2}$, and

$$\cos\pi\xi \simeq (1-4\xi^2)$$

$$(1+\cos 2\pi\xi) \simeq 2(1-2\xi)$$

$$\cos 2\pi\xi \simeq (1-4\xi)$$

for all values of ξ defined in the interval $0 \leq \xi \leq \frac{1}{2}$.

Then, $\bar{u}_h$ and $\bar{v}_h$ are found to be as follows:

$$\begin{aligned}(\bar{u}_h) = \Big\{ & G^2\left(\pi A_3 - \frac{\pi^2 \varsigma}{4Z}\right)\left[2-(1-\cos\phi_K)2\eta\right]\xi + \\ & + GH\left[\pi\left(A_5 - \frac{\pi\varsigma}{Z}\right)(1-2\eta) + A_6 2\pi\left(\sin\frac{\phi_K}{2}\right)\eta\right]\xi + \\ & + H^2\left(\pi A_3 - \frac{\pi^2\varsigma}{4Z}\right)(2)(1-2\eta)\xi \Big\}\end{aligned} \qquad (2.45a\text{-}b)$$

$$\begin{aligned}(\bar{v}_h) = \Big\{ & -B_D\phi_K\left(\cos\frac{\phi_K}{2}\right)\eta - G(\phi_K + B_2\phi_K)\left(\cos\frac{\phi_K}{2}\right)(1-4\xi^2)\eta - \\ & - G^2\left[B_4\phi_K\left(\cos^2\frac{\phi_K}{2} - \sin^2\frac{\phi_K}{2}\right) + \frac{\phi_K}{4Z}\sin^2\frac{\phi_K}{2}\right]2(1-2\xi)\eta + \\ & + GH\left[\left(\phi_K B_5 + \pi B_6 - \frac{\pi}{2Z}\right)\sin\frac{\phi_K}{2} + \left(\phi_K B_9 + \pi B_{10} - \frac{\pi}{2Z}\right)\left(\sin\frac{\phi_K}{2}\right)(1-4\xi)\right]\eta \\ & + H^2\left[\pi B_7 - \frac{\pi^2}{4Z\phi_K}\right](2)(1-2\xi)\eta\Big\}\end{aligned}$$

2.10. Dimensionless Form of the Potential Energy

In terms of the dimensionless coordinates and parameters used in the foregoing, the equations for the total potential energy of the shell system, Eqs. (2.8), (2.3), (2.6) and (2.7) are reduced to the following:

$$\bar{U} = \left(\bar{V}_s + \frac{2VW}{\phi_k} \bar{V}_b + 2z\bar{\Omega} \right) \tag{2.46}$$

in which

$$\bar{U} = \frac{2z}{EtR\phi_k L} U$$

$$\begin{aligned}
\bar{V}_s = 4\int_0^{\frac{1}{2}}\int_0^{\frac{1}{2}} \Big\langle \Big\{ & \Big[s\bar{u}_{,\xi} + \frac{s^2}{2z}(\bar{w}_{,\xi})^2 + \frac{1}{\phi_k}\bar{v}_{,\eta} + \bar{w} + \frac{1}{2z\phi_k^2}(\bar{w}_{,\eta})^2 \Big]^2 - \\
& -2\Big[s\bar{u}_{,\xi} + \frac{s^2}{2z}(\bar{w}_{,\xi})^2 \Big]\Big[\frac{1}{\phi_k}\bar{v}_{,\eta} + \bar{w} + \frac{1}{2z\phi_k^2}(\bar{w}_{,\eta})^2 \Big] - \\
& -\frac{1}{4}\Big[s\bar{v}_{,\eta} + \frac{1}{\phi_k}\bar{u}_{,\eta} + \frac{s}{z\phi_k}\bar{w}_{,\xi}\,\bar{w}_{,\eta} \Big]^2 \Big\} + \frac{1}{12z^3}\Big\{ \\
& \Big\{ \Big[s^2\bar{w}_{,\xi\xi} + \frac{1}{\phi_k^2}\bar{w}_{,\eta\eta} \Big]^2 - 2\Big[\frac{s^2}{\phi_k^2}\bar{w}_{,\xi\xi}\bar{w}_{,\eta\eta} - \frac{s^2}{\phi_k^2}(\bar{w}_{,\xi\eta})^2 \Big] \Big\} \Big\rangle d\xi\, d\eta
\end{aligned} \tag{2.47a-d}$$

$$\begin{aligned}
\bar{V}_b = 2\int_0^{\frac{1}{2}} \Big\langle & \Big\{ s(\bar{u}_{,\xi})_e + \frac{s^2}{2z}(\bar{w}_{,\xi})_e^2 + \frac{Vs^2}{2z}\Big[(\bar{w}_{,\xi\xi})_e \cos\frac{\phi_k}{2} - (\bar{v}_{,\xi\xi})_e \sin\frac{\phi_k}{2} \Big] \Big\}^2 + \\
& + \frac{V^2 s^4}{12z^4}\Big\{ \Big[\bar{w}_e \cos\frac{\phi_k}{2} - \bar{v}_e \sin\frac{\phi_k}{2} \Big]_{,\xi\xi} \Big\}^2 \Big\rangle d\xi
\end{aligned}$$

$$\bar{\Omega} = 4\int_0^{\frac{1}{2}}\int_0^{\frac{1}{2}} (\bar{P}_x\,\bar{u} + \bar{P}_\phi\,\bar{v} + \bar{P}_r\,\bar{w})\, d\eta\, d\xi$$

2.11. Derivation of the Algebraic Equations

For the various loading and support conditions, $\bar{u}$ and $\bar{v}$ can be obtained by substituting $\bar{u}_p$, $\bar{v}_p$, $\bar{u}_h$, and $\bar{v}_h$ derived in the preceding sections. The resulting expressions, $\bar{u}$ and $\bar{v}$, together with $\bar{w}$ expressed by Eq. (2.17) or Eq. (2.31a), are then substituted into the total potential energy expression $\bar{U}$ of Eq. (2.46). The latter quantity is then made stationary with respect to the undetermined parameters G and H, i.e.,

$$\frac{\partial \bar{U}}{\partial G} = 0$$

$$\frac{\partial \bar{U}}{\partial H} = 0 \qquad (2.48\text{a-b})$$

After carrying out the integration, Eqs. (2.48a-b) are transformed into two simultaneous non-linear algebraic equations of G and H which have the following form:

$$c_{30}G^3+c_{21}G^2H+c_{12}GH^2+c_{03}H^3+c_{20}G^2+c_{11}GH+c_{02}H^2+c_{10}G+c_{01}H+c_{00}=0$$

$$(2.49\text{a-b})$$

$$d_{30}G^3+d_{21}G^2H+d_{12}GH^2+d_{03}H^3+d_{20}G^2+d_{11}GH+d_{02}H^2+d_{10}G+d_{01}H+d_{00}=0$$

The coefficients c_{ij} and d_{ij}, related to the variables G^iH^j, are very complicated expressions, containing the shell and loading parameters, and are listed in Appendix II.

It may be pointed out that some of the coefficients of the simultaneous non-linear algebraic Eqs. (2.49a-b) are related. This is due to the fact that the equations are derived from making the total potential of the shell system stationary. Since the strain is a quadratic of displacements, the total potential of the shell system $\bar{U}$ must be a 4th degree polynomial of displacement parameters G and H in the following form:

$$\begin{aligned}\bar{U}(G,H)= {} & k_{40}G^4+k_{31}G^3H+k_{22}G^2H^2+k_{13}GH^3+k_{04}H^4+ \\ & + k_{30}G^3+k_{21}G^2H+k_{12}GH^2+k_{03}H^3+k_{20}G^2+k_{11}GH+k_{02}H^2+ \qquad (2.50) \\ & +k_{10}G+k_{01}H+k_{00}\end{aligned}$$

in which k_{ij} is the coefficient for term G^iH^j.

By making the total potential energy stationary:

$$\frac{\partial \bar{U}}{\partial G} = 4k_{40}G^3+3k_{31}G^2H+2k_{22}GH^2+k_{13}H^3+ +3k_{30}G^2+2k_{21}GH+k_{12}H^2+ +2k_{20}G+k_{11}H+k_{10} = 0 \qquad (2.51a\text{-}b)$$

$$\frac{\partial \bar{U}}{\partial H} = k_{31}G^3+2k_{22}G^2H+3k_{13}GH^2+4k_{04}H^3+ +k_{21}G^2+2k_{12}GH+3k_{03}H^2+ +k_{11}G+2k_{02}H+k_{01} = 0$$

When the coefficients of Eqs. (2.51a-b) are compared with Eqs.(2.49a-b) it becomes obvious that some of the coefficients in Eqs. (2.49a-b) are related in the following manner:

$$\begin{aligned} c_{21} &= 3d_{30} \\ c_{12} &= d_{21} \\ 3c_{03} &= d_{12} \\ c_{11} &= 2d_{20} \\ 2c_{02} &= d_{11} \\ c_{01} &= d_{10} \end{aligned} \qquad (2.52a\text{-}f)$$

Even though the realization of these relations, Eqs.(2.52a-f), has no great theoretical value, yet, in practice, it is of some importance. Since the generation of the coefficients c_{ij} and d_{ij} into a form adaptable to the computer involves very tedious computations, recognition of Eqs.(2.52a-f) will save labor or serve as a check when the coefficients are derived independently. This becomes even more important when a larger number of undetermined parameters are used.

Making use of the relations shown in Eqs. (2.52a-f), Eq. (2.49b) may be written as:

$$\left(\frac{1}{3}\right)c_{21}G^3+c_{12}G^2H+3c_{03}GH^2+d_{03}H^3+\left(\frac{1}{2}\right)c_{11}G^2+2c_{02}GH+d_{02}H^2+$$
$$+c_{01}G+d_{01}H+d_{00} = 0 \tag{2.53}$$

2.12. Solution of the Non-linear, Simultaneous Algebraic Equations

2.12.1. General: For a given set of load and geometric parameters, the coefficients c_{ij} and d_{ij} are simply constants. The resulting set of cubic equations are then solved by the Newton-Raphson iteration scheme programmed for the CDC 3600 computer at the Michigan State Computer center. In passing, it may be mentioned that the Gauss-Seidel method was tried but it failed to converge in some cases. The computer generates the numerical values of the coefficients as well as solves the equations. The method of solution is described in the following section:

2.12.2. Newton-Raphson Iteration: A normal system of algebraic equations,

$$f_1(x_1,\ x_2,\ x_3,\ \ldots\ x_i) = 0 \tag{2.54}$$
$$\vdots$$
$$f_i(x_1,\ x_2,\ x_3,\ \ldots\ x_i) = 0$$

can be expressed in matrix notation as

$$F(x) = 0 \tag{2.55}$$

The solution of Eq. (2.55) by the Newton-Raphson iteration procedure is as follows:

$$X_{n+1} = X_n - (J(X_n))^{-1}F(X_n) \tag{2.56}$$

in which $J(X_n)$ is the Jacobian matrix of the system of Eqs. (2.55) evaluated at X_n. The subscript n indicates the number of iterations. As pointed out by Henrici (7), (1962) and Zaguskin (23), (1961), the above procedure converges to the real solutions provided that X_o, the initially guessed solutions, are sufficiently close to the true solution and that $J(X_n)$ is non-singular. Thus the solutions of Eqs. (2.49a) and (2.53), when expressed in the form of the iterative Eq. (2.56), become:

$$(G)^m_{n+1} = (G)^m_n - (DH \times CC - CH \times DD)^m_n \Big/ (CG \times DH - CH^2)^m_n$$

(2.57a-b)

$$(H)^m_{n+1} = (H)^m_n - (-CH \times CC + CG \times DD)^m_n \Big/ (CG \times DH - CH^2)^m_n$$

The subscript n indicates the number of iterations while the superscript m indicates the number of load increments applied, and

$$(CC)^m_n = \left\{ \text{Left-hand side of Eq. (2.49a)} \right\}^m_n \tag{2.58a-b}$$

$$(DD)^m_n = \left\{ \text{Left-hand side of Eq. (2.53)} \right\}^m_n$$

with G and H evaluated at G^m_n and H^m_n, while $(CG)^m_n$, $(CH)^m_n$, $(DG)^m_n$ and $(DH)^m_n$ are partial derivatives of $(CC)^m_n$ and $(DD)^m_n$ with respect to G^m_n and H^m_n. They are given as follows:

$$(CG)^m_n = \frac{\partial}{\partial G}\left\{(CC)^m_n\right\} = (3c_{30}G^2+2c_{21}GH+c_{12}H^2+2c_{20}G+c_{11}H+c_{10})^m_n$$

$$(DG)^m_n = \frac{\partial}{\partial G}\left\{(DD)^m_n\right\} = (c_{21}G^2+2c_{12}GH+3c_{03}H^2+c_{11}G+2c_{02}H+c_{01})^m_n \qquad (2.59a\text{-}c)$$

$$(DH)^m_n = \frac{\partial}{\partial H}\left\{(DD)^m_n\right\} = (c_{12}G^2+6c_{03}GH+3d_{03}H^2+2c_{02}G+2d_{02}H+d_{01})^m_n$$

$$(CH)^m_n = \frac{\partial}{\partial H}\left\{(CC)^m_n\right\} = \frac{\partial}{\partial G}\left\{(DD)^m_n\right\} = (DG)^m_n$$

For a given shell system, under the first small increment of load, the shell behavior will be essentially linear, therefore, the solution of the linearized equations, G^1_L and H^1_L, obtained by setting all the non-linear terms of Eqs. (2.49a) and (2.53) equal to zero, will be very close to G^1 and H^1, the real solutions of Eqs. (2.49a) and (2.53). Therefore the linearized solutions, G^1_L and H^1_L are used as a first approximation applied in the iteration scheme outlined by Eqs. (2.57a-b);

i.e.,

$$G^1_1 = G^1_L$$
$$H^1_1 = H^1_L \qquad (2.60a\text{-}b)$$

After substituting Eqs.(2.60a-b) into Eqs.(2.57a-b) and starting the iteration, new values G^1_2 and H^1_2 are obtained, which are in turn substituted back into Eqs.(2.57a-b) to obtain G^1_3 and H^1_3. This iterative process will continue until G^1_{n+1} and H^1_{n+1} reach the value of $\hat{G}^1$ and $\hat{H}^1$, such that $|\hat{G}^1 - G^1_n| < 1 \times 10^{-9}$ and $|\hat{H}^1 - H^1_n| < 1 \times 10^{-9}$, simultaneously. $\hat{G}^1$ and $\hat{H}^1$ are considered to be the solutions to Eqs. (2.49a) and (2.53) with load increment equal to one unit. When the next increment of load is added, the initial guessed solutions G_o^2 and H_o^2 will be extrapolated linearly from $\hat{G}^1$, $\hat{H}^1$ and $\hat{G}^o$, $\hat{H}^o$. The latter quantities, $\hat{G}^o$, $\hat{H}^o$ are equal to zero as they correspond to the case of no load on the shell. It can be shown that,

$$G_o^2 = 2(\hat{G}^1 - \hat{G}^o) + \hat{G}^o \qquad (2.61a\text{-}b)$$

$$H_o^2 = 2(\hat{H}^1 - \hat{H}^o) + \hat{H}^o$$

In general, when the (m+1)th increment of load is added to the shell system, the initial guessed solutions G_o^{m+1} and H_o^{m+1} can be expressed as

$$G_o^{m+1} = 2(\hat{G}^m - \hat{G}^{m-1}) + \hat{G}^{m-1} \qquad (2.62a\text{-}b)$$

$$H_o^{m+1} = 2(\hat{H}^m - \hat{H}^{m-1}) + \hat{H}^{m-1}$$

and from the existence of a continuous solution of the problem, G_o^{m+1} and H_o^{m+1} will be very close to the real solutions, G^{m+1} and H^{m+1} , provided that the load increment chosen is sufficiently small. The iterative procedure of Newton-Raphson therefore converges rapidly to $\hat{G}^{m+1}$ and $\hat{H}^{m+1}$. However, if the load increment used happens to be not small enough so that the iterative procedure diverges, it is halved and the guessed solutions will also be reduced accordingly. The halving process will continue until a solution is obtained.

III. NUMERICAL RESULTS

3.1. Effect of Types of Load

As pointed out earlier, because of the inherent difficulty in dealing with loading that has a component in the circumferential direction, all the research work done on the large deflection behavior of cylindrical shell panels has been concerned with radial pressure only. However, for shell structures in civil engineering, such as cylindrical roof shells, the dead load and live load are the more common types of loading considered in design. It is therefore of interest to compare the behavior of a cylindrical shell with different types of loading.

Fig. 3.1. presents the load-deflection behavior of shells supported by rollers on all the edges and subjected to the three types of loading: radial load, live load and dead load. All shells have $\phi_k = 0.632$ and $S = 0.791$. Three sets of curves are shown for $Z = 100$, 125, and 150. These curves are plotted with the load parameters q_{LL}, q_{RL} or q_{DL} as the ordinate, and the dimensionless deflection $\frac{w_o}{t}$ as the abscissa, in which w_o is the deflection at the center of the shell.

It can be seen from the figure that for small deflections, (say $\frac{w_o}{t} < 0.5$) the load-deflection behavior is essentially linear.

With increasing load, however, the characteristics of non-linear behavior become evident. The slopes of the curves decrease over a large range of deflection -- indicating a loss of stiffness. After that, within the range of deflections considered, the stiffness may continue to decrease or begin to increase, depending upon the values of parameters used. For example, in the case of $Z = 150$, the stiffness of the shell continues to decrease. In fact, these curves all have a large "flat" portion. (For convenience of discussion, the loading corresponding to this flat portion of the curve will be referred to as the "buckling load.") However, for $Z = 100$, the curves begin to regain stiffness after some initial loss.

From Fig. 3.1. it is seen that for $Z = 150$, the buckling load for radial pressure is about 5% higher than that for live load and 10% higher than that for dead load. This may be explained qualitatively by noting that the radial component of load tends to keep the shell circular in shape while the tangential component tends to flatten the shell, and therefore contributes more to instability. A simple analysis shows that, by integrating the load functions of the three types of loading over a half section of the shell, the total resultant force in the radial direction for the three loading conditions are nearly the same. However, the dead load has a larger resultant of tangential component than that of the live load while the radial load has a zero tangential component.

It can be seen also from Fig. 3.1. that the differences in the stiffness of the shell subjected to different types of loads decrease as the value of Z is increased. This may be explained by noting that Z is essentially a curvature parameter, and the difference in the three types of loading is essentially due to the curvature of the shell surface. When Z becomes very large, the shell approaches a flat plate and the three types of loading become identically the same.

It might be pointed out also, that the effects of different types of load on the large deflection behavior are not great, because the shells considered have relatively small ϕ_k. When ϕ_k is large, the effects might be more pronounced than those shown in Fig. 3.1.

3.2. Effect of Shell Geometry

The following discussion is concerned with the effects of the geometric parameters on the behavior of shells supported by flexible beams on the longitudinal edges, and by rollers on the curved edges. Only the dead load case is considered. As before, the behavior of the shells is described in terms of load-deflection curves.

3.2.1. Effect of Z (radius/thickness ratio): From the figure presented in the preceding section, it can be seen that the shell is stiffer for smaller values of Z. Additional data on the influence of Z are presented in Fig. 3.2. in which the shells are supported by edge beams (V = 10, W = 0.025). Five values of Z, ranging from

75 to 175 are considered. As before, it is seen that the buckling load is lower for higher values of Z. This general result agrees with the physical intuition that the thinner the shell (or flatter the curvature), the smaller would be the buckling load.

In order to better relate the results to practical cases, the shell considered in Fig. 3.2. may be interpreted as having the following dimensions:

R = 60'-0", L = 76'-0", a = 41" and b = 18".

For the case of Z = 175, t is equal to 4.1", and E = 3 x 10^6psi; the buckling load is then equal to 340 psf. If Z =100, and t is equal to 7.2", then the buckling load is 880 psf. Whereas, if Z = 75 so that t becomes 9.6", the shell becomes very stiff, and does not buckle even when the load has been increased to four times the buckling load for t = 4.1". This nonlinear phenomenon is different from the linear relationship between the buckling load and Z implied in the ASCE Manual No. 31.

3.2.2. Effect of ϕ_k : Obviously, the size of the opening angle of a shell, ϕ_k, influences the buckling strength of the shell. Fig. 3.3. presents the effect of ϕ_k on the buckling strength of shells having the following properties:

S = 0.791, V = 10, W = 0.025, Z = 125 and 150.

Three values of ϕ_k are considered: 0.5, 0.632 and 0.8. It is seen that the buckling strength of shells increases with an increase of ϕ_k.

(For $\phi_k = 0.8$, the shell did not buckle at all). For the case Z = 150, the shell could be interpreted to be one having L = 63'-4", R = 50'-0", t = 4", a = 40", b = 15" and E = 3 x 10^6psi. For this shell, if $\phi_k = 0.5$ (roughly 29°), the buckling dead load is 200 psf. If $\phi_k = 0.632$ (roughly 36°), the buckling load becomes 430 psf. When $\phi_k = 0.8$ (roughly 46°), the shell becomes so stiff that even when p_{DL} is equal to 1,250 psf. it is still stable.

3.2.3. <u>Effect of S (radius/length ratio)</u>: The effect of S on shell behavior is presented in Fig. 3.4. in which the shells considered have the following properties:

$\phi_k = 0.632$, Z = 125, W = 0.025, V = 10,

and S takes on five different values. It is seen that the buckling load increases with an increase of the value of S.

If t is again assumed to be 4", then the shells considered in Fig. 3.4. correspond to those having the following dimensions:

$\phi_k = 0.632$, R = 41'-8", a = 40", b = 15".

If L is equal to 88'-0" (corresponds to S = 0.475) and E = 3 x 10^6psi, the buckling load is p_{DL} = 70psf. If L is decreased to 66'-0" (corresponds to S = 0.632), the buckling dead load is 300 psf. If L is decreased to 53'-0 (corresponding to S = 0.791), the buckling dead load becomes 580 psf. These results simply indicate that if all other parameters are held constant, a decrease in the span length of the shell would result in an increase of the buckling strength.

3.2.4. Effect of Edge Beams: The role of the edge beams is represented by the depth parameter V $(=\frac{a}{t})$ and the width parameter $W(=\frac{b}{R})$. The influence of V and W are shown in Fig. 3.5. and Fig. 3.6., respectively. In these two figures, the following shells are considered:

$\phi_k = 0.632$, $S = 0.791$, $Z = 100$, 125, and 150.

In Fig. 3.5., W is held constant at 0.025 and V takes on the values of: 5, 10, 15 and 20. It is seen that for a given Z, the initial deflection is essentially independent of V. However, as the deflection increases to a certain value (depending on the value of Z), the influence of V becomes more conspicuous; it is more pronounced for smaller values of Z. Furthermore, as V increases in value, the shell becomes stiffer.

In Fig. 3.6., V is held constant at 10, and three values of W are assumed: 0.0125, 0.025 and 0.05. The behavior pattern is similar to that just discussed for Fig. 3.5. That is, the influence of W becomes apparent only after the deflection assumes a substantial magnitude. This influence is also larger for smaller values of Z. This case may be interpreted as indicating that the influence of the edge beam is greater for thicker shells. This behavior might be explained by the fact that for thinner shells, the stiffness of the edge beam is probably not called on to play its part, even when the shell is undergoing large deflections.

3.3. Comparison of Results

The method of analysis used in this study is an approximate one and involves a number of assumptions. It is, therefore, natural to question the accuracy of the results obtained. In general, the assessment of the accuracy of an approximate method of this type is to compare results with known exact solutions. As discussed in the Introduction, for the case of nonlinear behavior of cylindrical shell panels, available solutions are extremely scarce; besides, they are all approximate solutions of the Rayleigh-Ritz type. In fact, so far as is known to the author, Ref. (11) contains the only existing data that may be used for comparison in order to give some indication of the accuracy of the results of this study. Before presenting this comparison, however, a linear problem will be examined.

Consider a concrete shell simply supported by edge beams with the following dimensions: R = 33'-4", L = 111'-0", $\phi_k = 30^o$, t = 4", a = 60" and b = 8". The load is derived from a live load of 25 psf and the weight of the shell itself. The solutions of this structure in terms of N_x and N_ϕ at the mid-span of the shell for different values of ϕ are plotted in Fig. 3.7. It might be pointed out that in this case, the linear version of the solution (by dropping out the non-linear terms of G and H in Eqs. (2.49a) and (2.53)) is very close to the non-linear solutions. This is, of course, to be expected since the deflections are small. The linear response of the same shell has also been discussed in ASCE Manual No. 31 (1) (page 60). For all practical purposes, the solutions therein may be considered as exact, and they are also graphed in Fig. 3.7. It can be seen that results corresponding to the present analysis differ from the ASCE Manual solution only by about 1% at the crown. However, the agreement is not as good for points closer to the edge of the shell. Nevertheless, in view of the gross approximation used in the present analysis, the differences indicated in Fig. 3.7. should not be considered as being large.

For a comparison involving a non-linear problem, consider a shell loaded radially and supported by rollers on all its edges. Limiting to $\phi_k < 0.2$, and $\phi_k S = 0.5$, the load-deflection curves for different values of $\phi_k^2 Z$ are calculated and presented as solid curves in Fig. 3.8., in which the load parameter $(q_{RL} Z^4 \phi_k^4)$ is plotted against $\frac{w_o}{t}$. Also, shown as dotted lines in Fig. 3.8. are the results obtained by Kornishin and Mushtari, (11) for the same shell. As mentioned in the Introduction, the latter results were obtained by applying the method of Bubnov and Galerkin to the compatibility equation and the radial equilibrium equation. It is seen that the solutions obtained by the two procedures seem to differ appreciably. Depending on the value of $\phi_k^2 Z$, the buckling loads corresponding to the present analysis are approximately

10% to 70% higher than those indicated by Ref. (11), the discrepancy being smaller for smaller values of ${\phi_k}^2 Z$.

It should be noted that the results of Ref. (11) were obtained employing six undetermined parameters in the assumed functions, while in this study, only two undetermined parameters have been used. Therefore, it is probably reasonable to assume that for the problem considered the numerical results of Ref. (11) would be more accurate. It may appear that the difference between the two are substantial. It should be borne in mind, however, that the procedure used herein is devised to handle more realistic problems (particularly from the point of view of concrete shell structures) to which the technique used in Ref. (11) cannot be applied. Furthermore, against the background of the present state of knowledge of large deflection behavior of shells, as discussed in the Introduction and later in the Conclusion, this difference may not be as significant as it seems at first glance.

IV. SUMMARY AND CONCLUSION

4.1. Summary

A method has been developed to study analytically the non-linear behavior of elastic thin cylindrical shells. The shells are supported by rollers on all the edges or by rollers on the curved edges and flexible beams on the longitudinal edges. Three types of loading are considered: a uniform radial pressure, a uniform live load, and a uniform dead load.

The method of analysis is based on a large deflection theory of thin shells by including the quadratic terms $(\frac{\partial w}{\partial x})^2$ and $(\frac{\partial w}{R\partial\phi})^2$ in the strain tensor. The variational problem resulting from an application of the principle of stationary potential energy, is solved approximately by the method of Rayleigh-Ritz. A first harmonic approximation with two undetermined parameters, is chosen to represent the radial displacement function w. The longitudinal and circumferential displacement functions u and v are considered to consist of two parts: u_p, v_p and u_h, v_h. The functions u_p and v_p are chosen to be the particular solutions of the equation of equilibrium in the longitudinal and circumferential directions, respectively. The functions u_h and v_h are homogeneous solutions to $\nabla^4 u_h = \nabla^4 v_h = 0$, so that the sums $u = u_p + u_h$ and $v = v_p + v_h$ satisfy approximately the geometric and natural boundary conditions.

By applying these approximating functions to the Rayleigh-Ritz procedure, a set of two simultaneous algebraic cubic equations are obtained. Using a high speed digital computer, these equations are solved by the iteration scheme of Newton-Raphson. For a given shell and loading type, a load-deflection curve is obtained from a series of solutions corresponding to a range of load intensity. The curve is, in general, non-linear. It is indicated that after a certain range of essentially linear behavior, the stiffness of the shell decreases. Depending upon the values of the parameters of the system, the shell may or may not buckle. (Buckling is considered to have occurred if the shell undergoes substantial displacement with little change in load magnitude.)

By a repeated application of the above procedure for different values of shell parameters, a number of load deflection curves are obtained. From these numerical results, the principal findings may be summarized as follows:

Among the three loading conditions considered, the shell has the lowest stiffness (or buckling load) for the dead load case. The shells have lower stiffness or buckling loads for: smaller values of the opening angle, ϕ_k, smaller values of the radius to length parameter, S, larger values of the radius to thickness parameter, Z, and for smaller edge beams.

4.2. Concluding Remarks

In the past, the elastic stability of thin shells, treated either as a linear eigen-value problem or a non-linear large deflection problem, had been formulated in such a way that the boundary conditions were assumed not to play an important role in the behavior of the system. (2), (1947) and (9), (1941). Recently it was pointed out that the degree of constraint offered by the boundary could be a significant factor. (15), (1961) and (19), (1962). This is further demonstrated by the following comparison.

If one considers a shell loaded radially and having the following parameters: $S = 0.91$, $\phi_k = 0.632$, $Z = 100$, and the shell is simply supported on the curved edges and clamped along the longitudinal edges, the radial buckling load has been found by Sunakawa and Uemura (20), (1960) to be: $q_{RL} = \frac{10,800\text{psf}}{E}$. However, if the boundary conditions are changed to roller supports on all edges, the buckling load reduced to $q_{RL} = \frac{2000\text{psf}}{E}$ (obtained by the procedure used herein). Thus, it is noted that the different boundary conditions lead to a difference in buckling load of 500%!

The aspect of boundary condition on shell buckling has not been emphasized in the discussions of Stability of Roof Shells in the ASCE Manual No. 31 (1). In fact, the manual stated that for a long roof shell, N_x being the predominant force, the buckling characteristics are analogous to those of a curved panel stiffened at the edges subjected to axial compression; thus, the actual character of the boundary supports never enters into consideration. Such an assumption obviously oversimplifies the problem, as it should be clear from the preceding. That is, the buckling strength of a roof shell depends significantly on the degree of restraint offered by the supports.

Therefore, in the design of a roof shell, if the buckling problem is to be investigated, the actual boundary conditions should be duly taken into account. The method described in this thesis, admittedly approximate, may be used for that purpose.

4.3. Suggested Future Work

As a possible extension of the present work, it is natural to consider the use of the present approach by including higher harmonics in the assumed displacement functions. However, it is emphasized that the amount of labor involved in the analysis is immense. Therefore, before making such an effort, it seems desirable to conduct an experimental investigation of the problem. The results of such an investigation may provide a more definite idea about the accuracy of the present approach. Furthermore, observations on the actual physical behavior may suggest a more intelligent choice of the assumed deflection functions for the Rayleigh-Ritz method.

V. BIBLIOGRAPHY

1. American Society of Civil Engineers, "Design of Cylindrical Concrete Shell Roofs," Manuals of Engineering Practice No. 31, 1952.

2. Batdorf, S. B., "A Simplified Method of Elastic-Stability Analysis for Thin Cylindrical Shells," NACA Rep. 874, 1947.

3. Chung, K. P. and Veletsos, A. S., "A Study of Two Approximate Methods of Analyzing Cylindrical Shell Roofs," Structural Research Series No. 258, University of Illinois, October 1962.

4. Donnell, L. H., "A New Theory for the Buckling of Thin Cylinders under Axial Compression and Bending," Trans. ASME, Vol. 56, p. 795, 1934.

5. Finkel'shtein, R. M., "On a Problem in the Statics of Thin Cylindrical Plates" (in Russian), Izv. Akad. Nauk SSSR, Otd. Tekb. Nauk No. 5, pp. 130-140, May 1956.

6. Fung, Y. C. and Sechler, E. E., "Instability of Thin Elastic Shells, "Structural Mechanics, Proceedings of the First Symposium on Naval Structural Mechanics, Pergamon Press, New York, pp. 115-168, 1960.

7. Henrici, Peter, "Lecture Notes on Elementary Numerical Analysis," John Wiley and Sons, 1962.

8. Karakas, J. and Scalz, M., "Test Load of Shell Fails at Design Load," Civil Engineering, March 1961.

9. Kármán, Th. von, and Tsien, H. S., "The Buckling of Thin Cylindrical Shells under Axial Compression," Journal of the Aeronautical Sciences, Vol. 8, No. 8, p. 303, June 1941.

10. Koiter, W. T., "Buckling and Post-Buckling Behavior of a Cylindrical Panel under Axial Compression," Nat. Lucht Lab., Amsterdam Rap. 5, p. 476, 1956.

11. Kornishin, M. S. and Mushtari, Kh. M., "A Certain Algorithm of the Solution of Non-Linear Problems of the Theory of Shallow Shells," (English Translation of Prikl. Mat. Mekh.) 23, 1, Pergamon Press, New York, pp. 211-218, 1959.

12. Langhaar, H. L., "General Theory of Buckling," Applied Mechanics Reviews, Vol. 11, No. 11, Nov. 1958.

13. Langhaar, H. L., "Energy Methods in Applied Mechanics," John Wiley and Sons, New York, 1962.

14. Mushtari, Kh. M. and Galimov, K. Z., "Non-linear Theory of Thin Elastic Shells," (English Translation). Published for the National Science Foundation and the National Aeronautics and Space Administration by the Israel Program for Scientific Translation. 1961.

15. Nachbar, W. and Hoff, N. J., "On Edge Buckling of Axially-Compressed, Circular Cylindrical Shells," SUDAER No. 115 (NsG 93-60), Dept. Aero. Eng., Stanford University, Nov. 1961.

16. Nash, W. A., "Recent Advances in the Buckling of Thin Shells," Applied Mechanics Review, Vol. 13, No. 3, March 1960.

17. Novozhilov, V. V. and Finkel'shtein, R. M., "On the Error of Kirchhoffs' Hypothesis in the Theory of Shells," Prikl. Nat. Mekh. Vol. 7, No. 5, 1943.

18. Soderquist, A. B. T., "Experimental Investigation of Stability and Postbuckling Behavior of Stiffened Curved Plates," University of Toronto, Inst. Aerophys., TN 41, 1960.

19. Stein, M., "The Effect on the Buckling of Perfect Cylinders of Prebuckling Deformations and Stresses Induced By Edge Support," NASA Technical Note D 1510, 1962.

20. Sunakawa, M. and Uemura, M., "Symmetrical Buckling of Cylindrical Shells under External Pressure," Aeronautical Research Institute, University of Tokyo, Report No. 356, Mat 1960.

21. Timoshenko, S. P. and Gere, J. M., "Theory of Elastic Stability," McGraw Hill Book Company, 1961.

22. Timoshenko, S. and Woinowsky-Krieger S., "Theory of Plates and Shells," 2nd ed., McGraw Hill, New York, 1961.

23. Zaguskin, V. L., "Handbook of Numerical Methods for the Solution of Algebraic and Transcendental Equations," (English Translation), Pergamon Press, 1961.

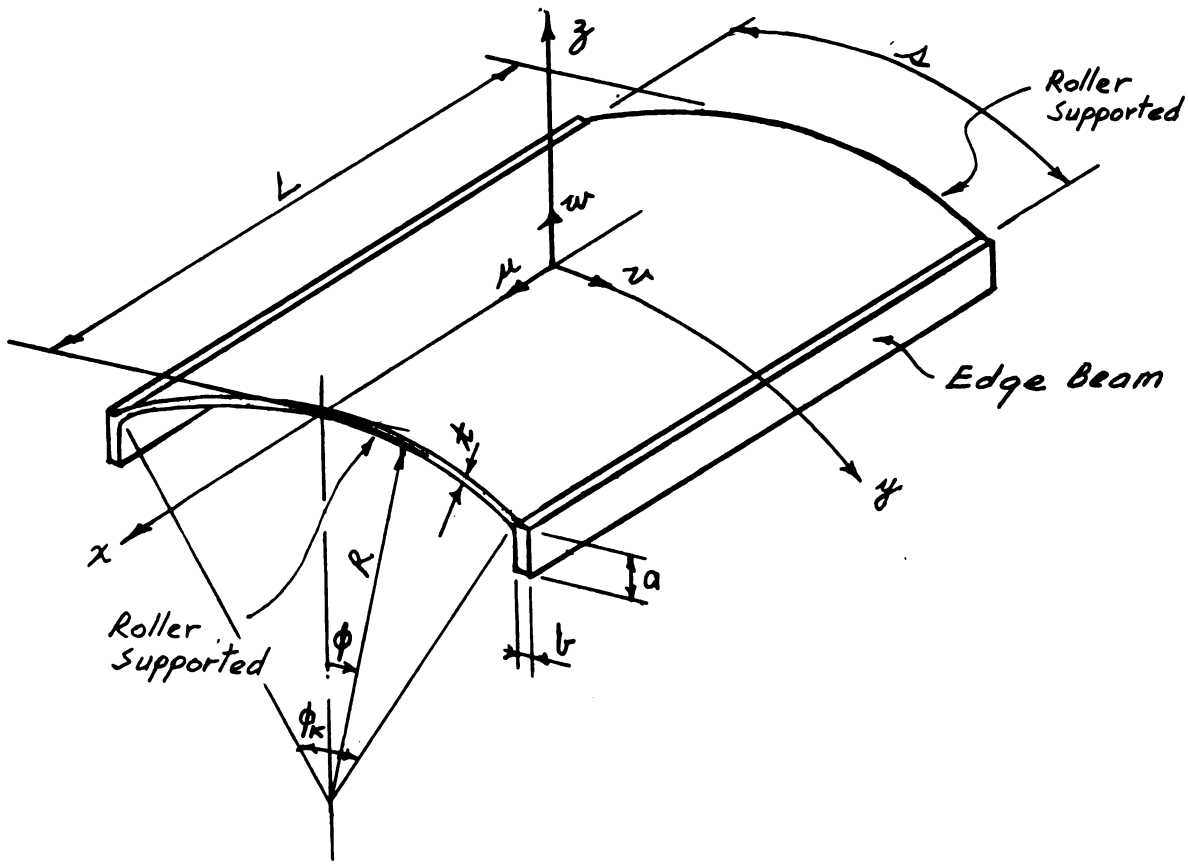

(a) Shell System Considered

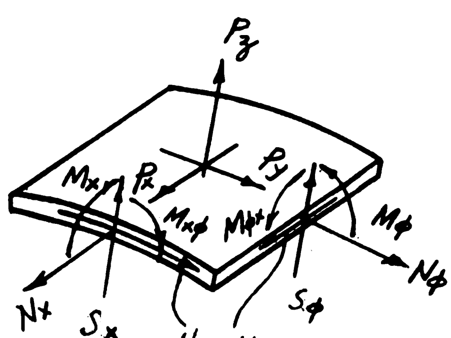

(b) Force System Considered

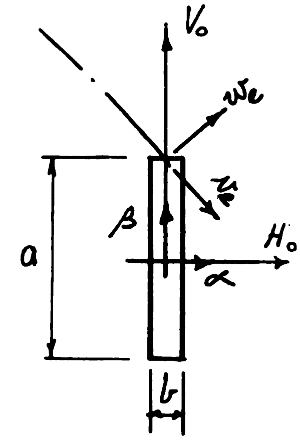

(c) Edge Beam Cross Section

Fig. 2.1. Cylindrical Shells Supported by Flexible Beams on Longitudinal Edges and by Rollers on the Curved Edges

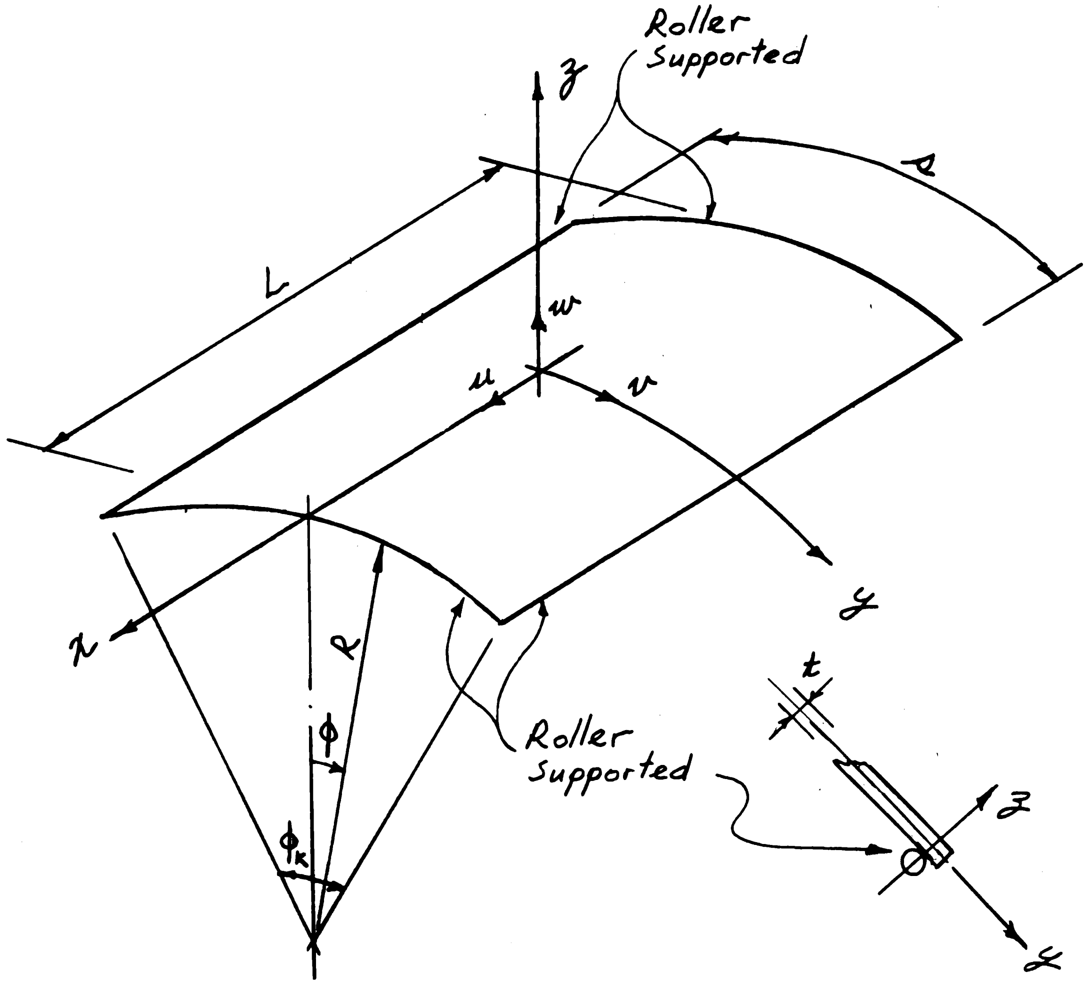

Fig. 2.2. Cylindrical Shells Supported by Rollers on All Edges

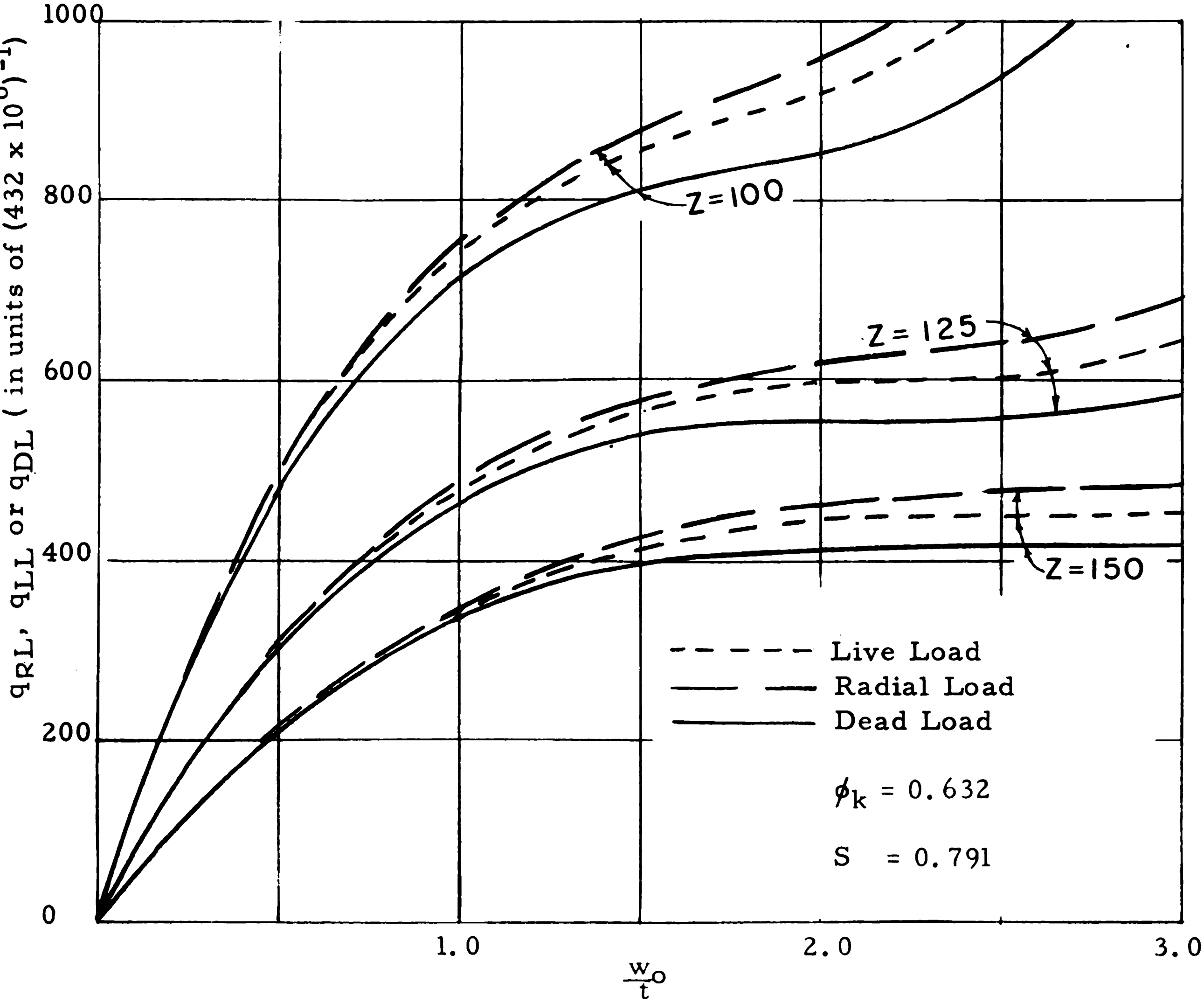

Fig. 3.1. Effect of Types of Load (Roller Supported)

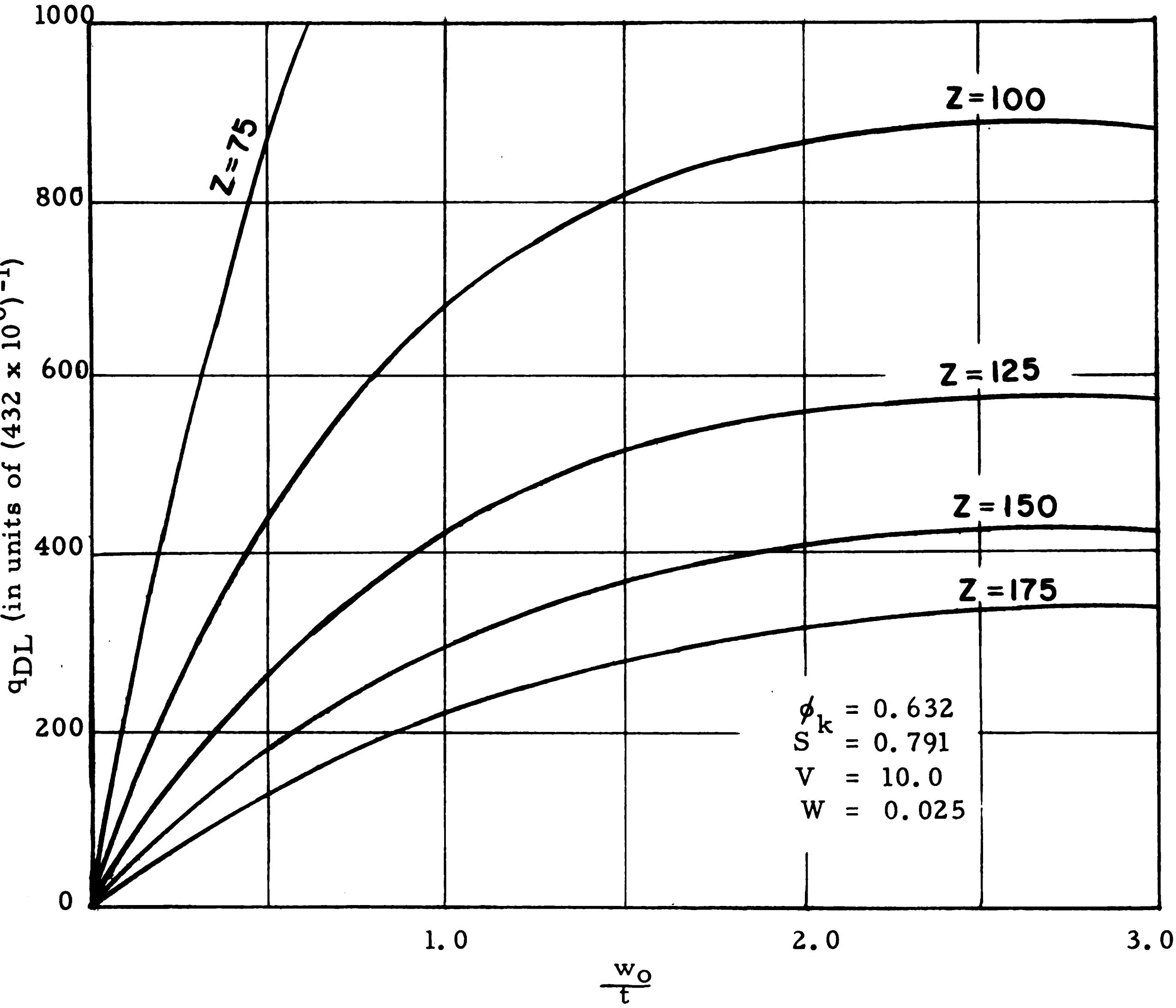

Fig. 3.2. Effect of Z ($Z = \frac{R}{t}$). (Beam Supported)

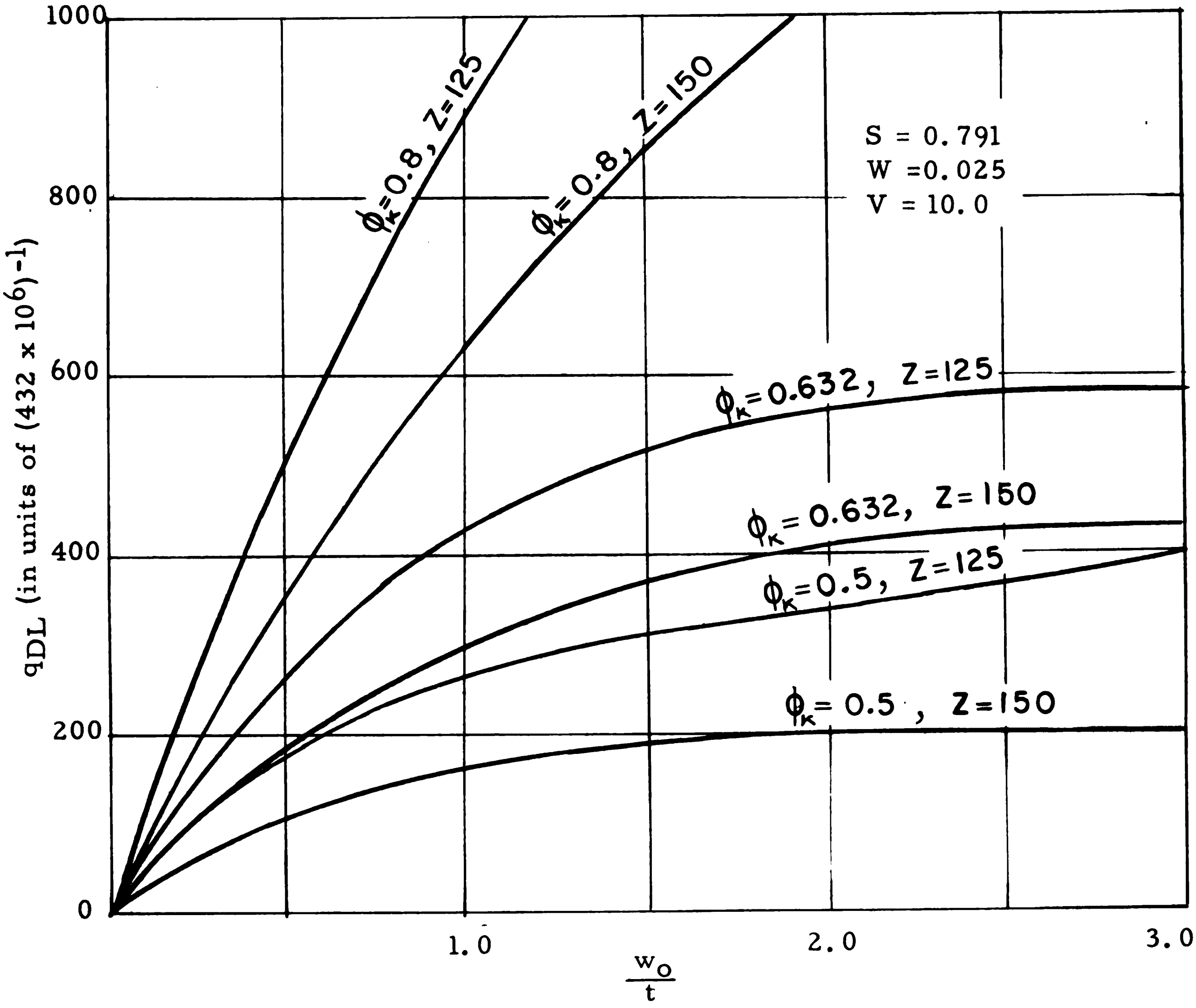

Fig. 3. 3. Effect of ϕ_k. (Beam Supported)

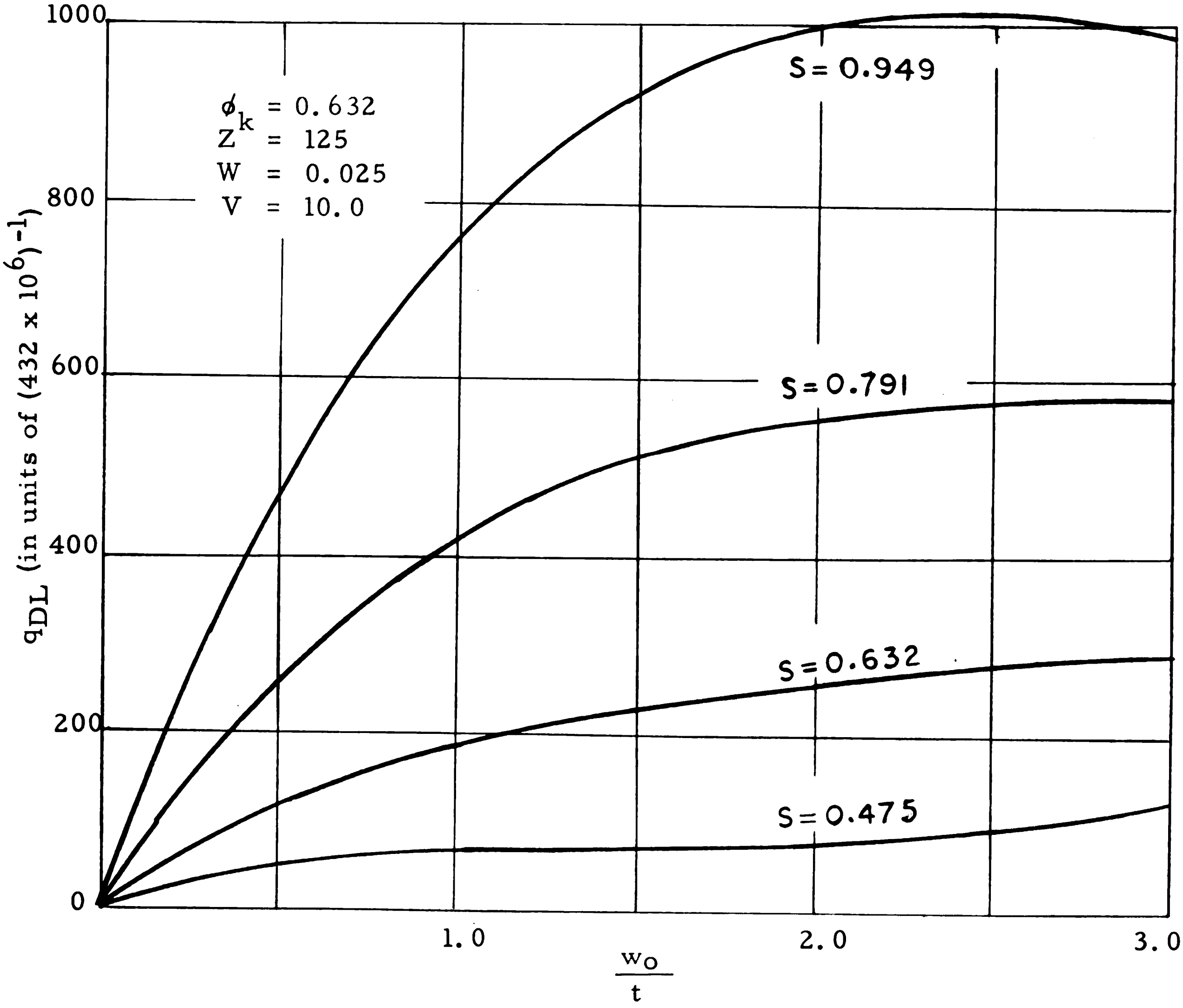

Fig. 3.4. Effect of S ($S = \frac{R}{L}$). (Beam Supported)

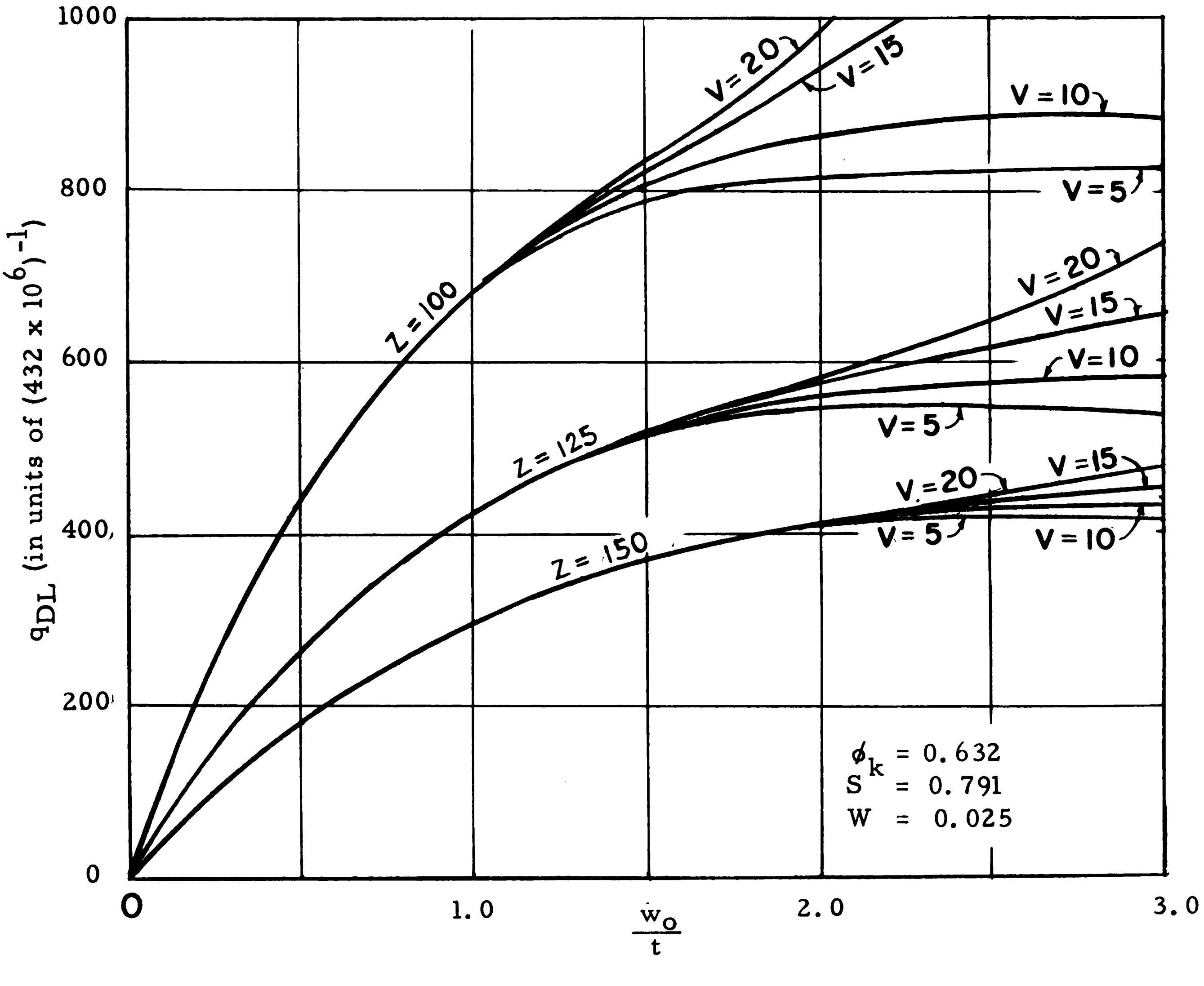

Fig. 3.5. Effect of V ($V = \frac{a}{t}$). (Beam Supported)

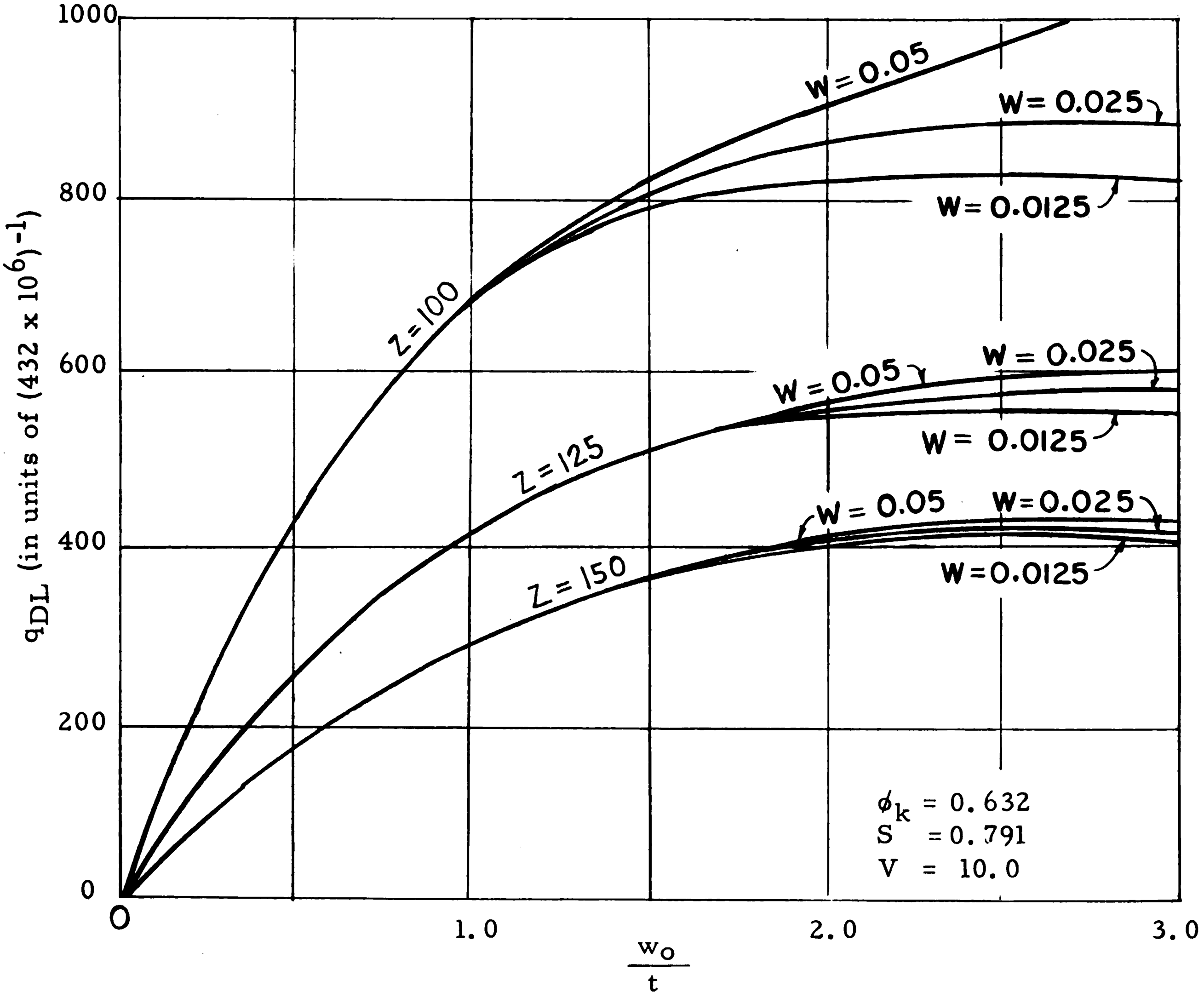

Fig. 3.6. Effect of W ($W = \frac{b}{R}$). (Beam Supported)

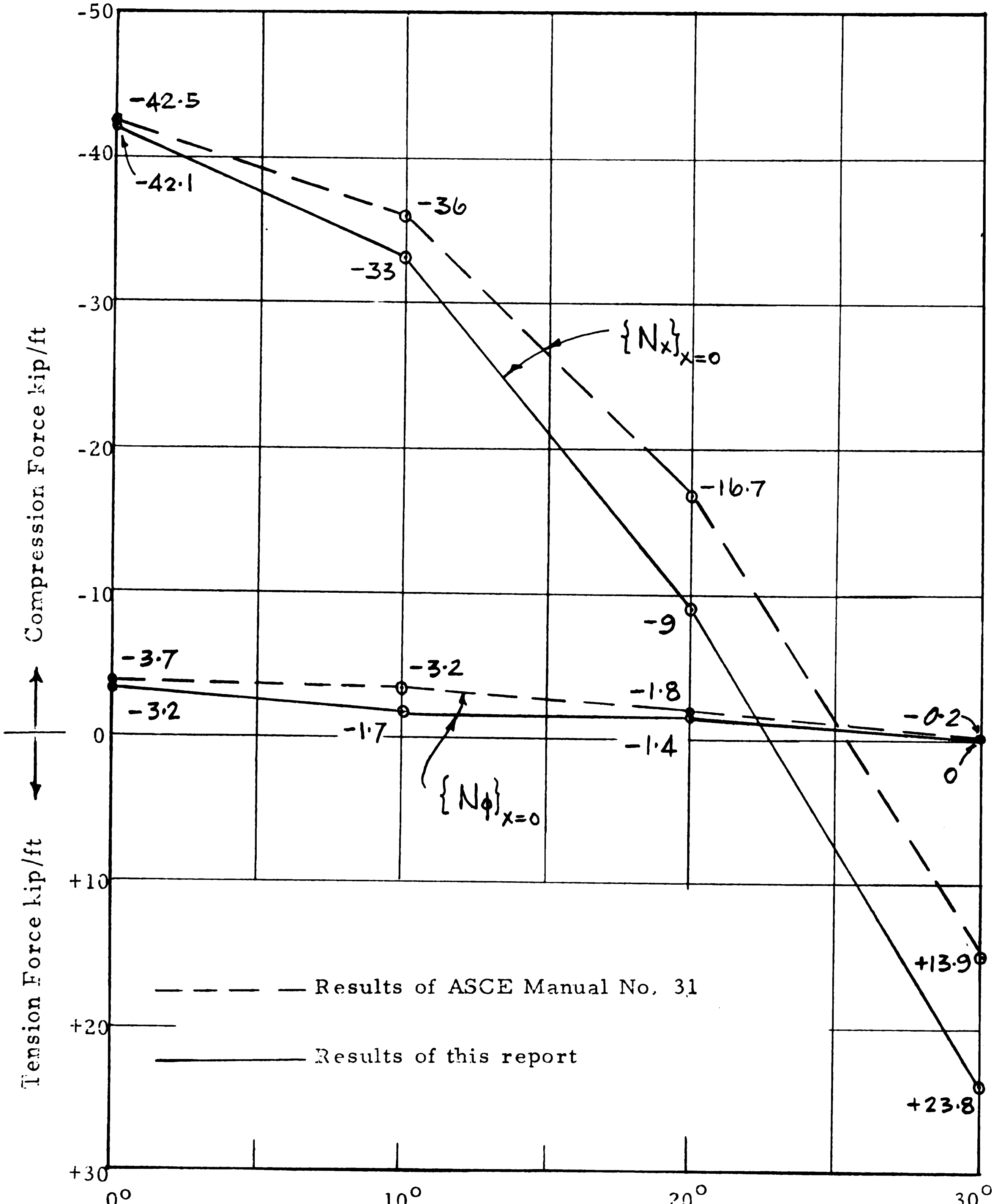

Fig. 3.7 Comparison of N_x and N_ϕ (Beam supported shell)

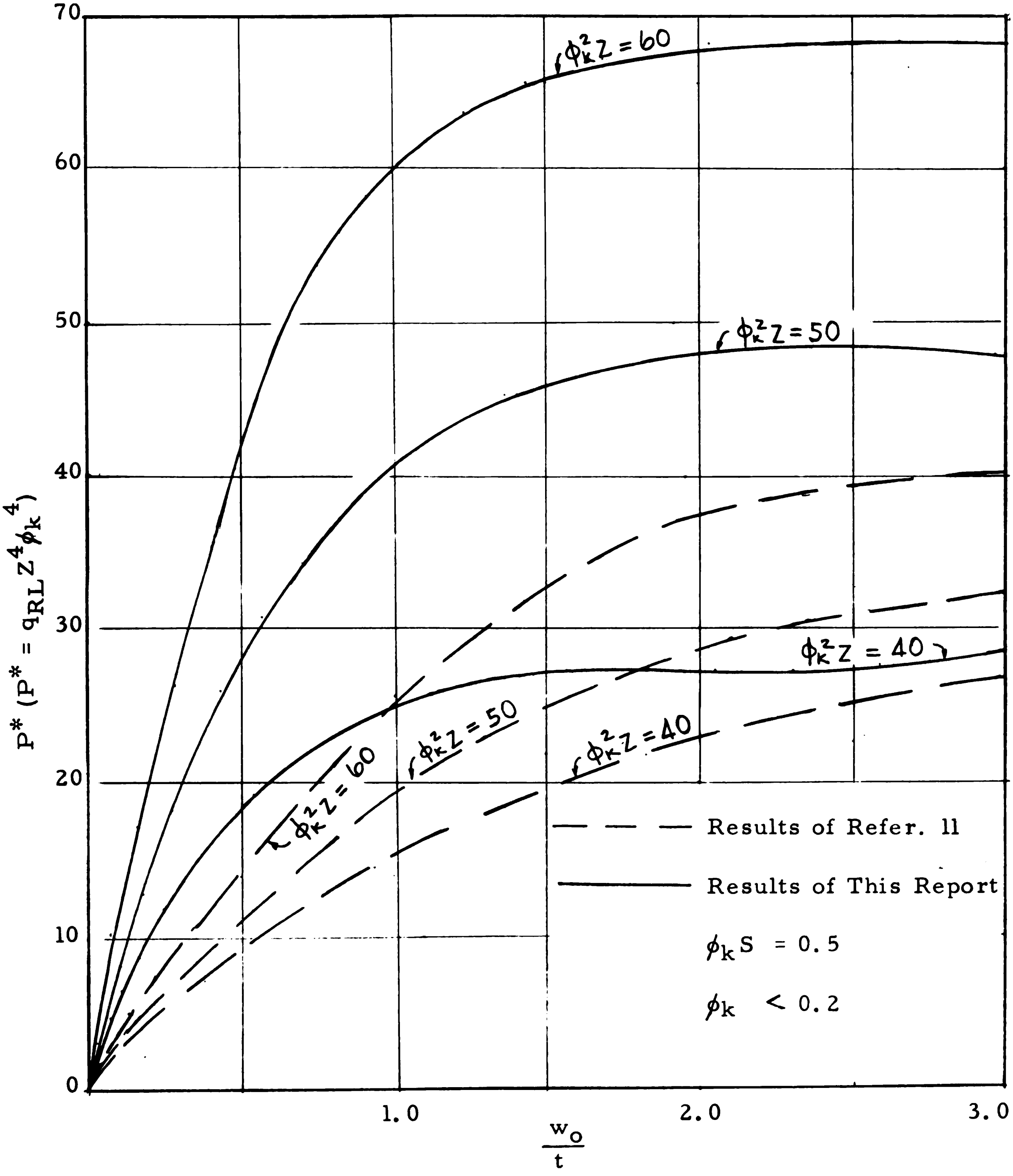

Fig. 3.8. Comparison of Results of This Report with Reference 11 (Roller Supported)

APPENDIX I

COMPARISON OF TWO CHOICES OF DISPLACEMENT FUNCTIONS

This appendix gives the comparison of the solutions obtained by a set of approximating displacement functions which do not satisfy the natural boundary conditions, and by those which satisfy the natural boundary conditions approximately. The comparison is shown in Fig. A.1. in the form of load-deflection curves for shells roller supported, loaded radially.

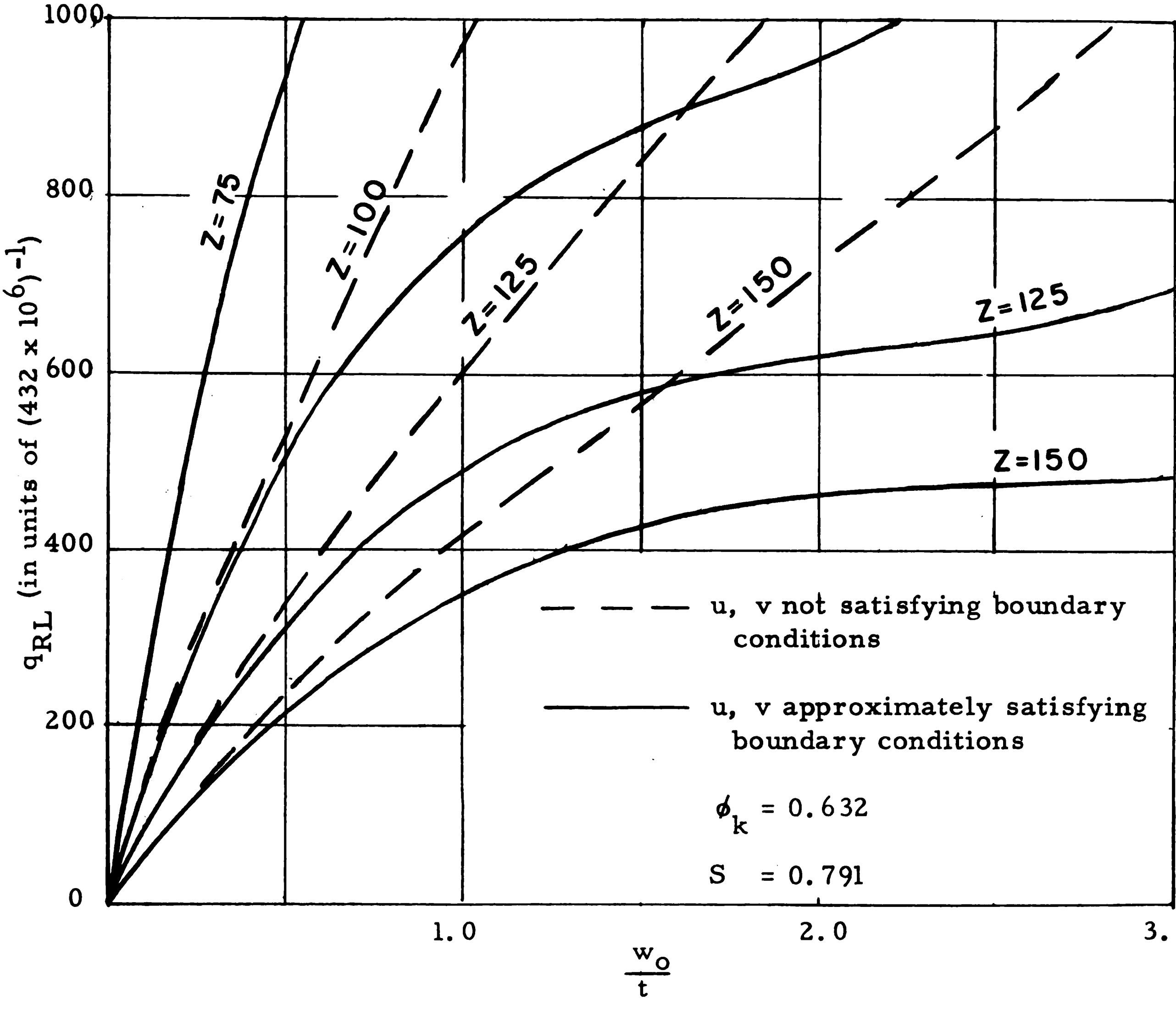

Fig. A.1. Comparison of Load-Deflection Relations for Two Choices of Displacement Functions (Roller Supported)

APPENDIX II.

COEFFICIENTS OF EQUATIONS (2.49a-b)

A.2.1. General

The coefficients of Eqs. (2.49a-b) are given below in terms of the Fortran language (see, for example, McCracken, D. D., "A Guide to Fortran Programming," John Wiley and Sons 1961). The definitions of the Fortran variables used are given in Section A.2.2., and then followed by the presentation in Section A.2.3. of the coefficients c_{ij} and d_{ij}. It is noted that the materials presented subsequently are direct printouts from the original computer program. This is done in order to avoid possible errors in transcribing these lengthy expressions, as well as for convenience of reproduction.

A2.2 ***** LIST OF FORTRAN VARIABLES. *****

```
C          **PARAMETERS OF SHELL.**
C      XBAR=RADIUS TO LENGTH RATIO, S.
C      Z1  =RADIUS TO THICKNESS RATIO, Z.
C      P   =OPENING ANGLE.
C      V   =EDGE BEAM DEPTH TO THICKNESS RATIO.
C      WBAR=EDGE BEAM WIDTH TO RADIUS RATIO.
C      U   =POISSON,S RATIO
C      DL= LOAD INTENSITY OF RADIAL PRESSURE, LIVE LOAD, OR DEAD LOAD.
C      QR  =DIMENSIONLESS LOAD PARAMETER, DL/E
C      E   =YOUNGS MODULUS
C          **FORTRAN VARIBLES USED IN COMPUTER PROGRAM**
C      DDL =LOAD INCREMENT.
C      DOADIN=LOAD INCREMENT COUNTER, THAT IS  THE NUMBER OF LOAD INCREMENT
C             ACCUMULATED.
       QR=DL/E
       Z=12.*P*P*Z1
       Y=1./Z1/P
       X=XBAR*P
       W=V*V*V*WBAR
       F2=PI/P
       F3=PI*X
       F4=PI*P
       F5=P/X
       F6=PI/X
       F12=PI*PI/P/P
       F13=PI*PI*X*X
       F14=PI*PI*P*P
       F23=PI*PI*X*PI*X*X
       F31=0.5/(F2-1.0)**2
       F32=0.5/(F2+1.0)**2
       F33=0.5/(F12-1.0)
       A1=((P*P -U*F13        )*F4  *X)/(P*P +F13        )**2
       A2=((1.0-U*X*X )*P*X)/(PI*(1.0+X*X )**2)
       A3=(PI**2*X**2-U*P**2)/(8.0*PI*X)
       A4=((X**2-U)*PI)/(8.0*X)
       A5=((((4.0*F13        )+(PI*PI+P*P ))**2+4.0*F14        )*F3  *((2
        .0*F13        +PI*PI+P*P )**2+2.0*F13        *(2.0*F13-
        U*(PI*PI+P*P )))-8.0*F3*F4*F4     *((4.0*F13        +PI*PI+P*P )*
         (2.0*(2.0+U)*F13         +P*P +PI*PI)))/(((4.0*F13        +PI*PI
         +P*P )**2+4.0*F14        )**2-(4.0*F4  *(4.0*F13        +PI*PI+
         P*P ))**2)
```

```
A6=( (F3  *(4.0*F4  *(4.0*F13       +PI*PI+P*P )))*( (2.0*F13
      +PI*PI+P*P )**2+2.0*F13       *(2.0*F13       -U*(P*P -PI
   *PI)))-2.0*F3*F4   *((4.0*F13       +PI*PI+P*P )**2+4.0*F14
       )*(2.0*(2.0+U)*F13       +PI*PI+P*P ))/(((4.0*F13
   +PI*PI+P*P )**2+4.0*F14       )**2-(4.0*F4  *(4.0*F13       +
   PI*PI+P*P ))**2)
A7=PI*X/8.0
A20=2.0*(A3*F3-0.25*F13)
B2=-((P*P +(2.0+U)*F13       )*P*P )/(P*P +F13       )**2
B3=-((1.0+(2.0+U)*X*X )*P/(PI*(1.0+X*X )**2))
B4=(P*P -U*F13       )/(8.0*P)
B5=(((PI*PI+P*P )**2+4.0*F14       )*(P*P *(3.0* PI*PI+P*P )-U*(
  F13       )*(PI*PI+3.0*P*P ))*(PI/2.0)-(2.0*PI*F14    *(PI*PI+P*
  P ))*(PI*PI+3.0*P*P -U*X*X *(3.0*PI*PI+P*P )))/(((PI*PI+P*P
  )**2+4.0*F14       )**2-(4.0*F4  *(PI*PI+P*P ))**2)
B6=(((PI*PI+P*P )**2+4.0*PI*PI*P*P )*(PI*PI*(PI*PI+3.0*P*P )-U*F13
       *(3.0*PI*PI+P*P ))*0.5-(2.0*PI*PI*(PI*PI+P*P ))*(P*P
  *(3.0*PI*PI+P*P )-U*F13       *(PI*PI+3.0*P*P )))*P/(((PI*PI+P*P
   )**2+4.0*F14       )**2-(4.0*F4  *(PI*PI+P*P ))**2)
B7= PI*(1.0-U*X*X )/8.0
B8=P/8.0
B9=(((4.0*F13       +PI*PI+P*P )**2+4.0*F14       )*((2.0*F13
      +P*P )**2+P*P *(4.0*F13       +3.0*PI*PI)-U*F13       *
   (PI*PI-P*P ))*PI/2.0-(4.0*F4  *(4.0*F13       +PI*PI+P*P ))*
   ((2.0*F13       +PI*PI)**2+PI*PI*(4.0*F13       +3.0*P*P )+
   U*F13       *(PI*PI-P*P ))*P/2.0)/(((4.0*F13       +PI*PI+P
   *P )**2+4.0*F14       )**2-(4.0*F4  *(4.0*F13       +PI*PI+
   P*P ))**2)
B10=(((4.0*F13       +PI*PI+P*P )**2+4.0*F14       )*((2.0*F13
       +PI*PI)**2+PI*PI*(4.0*F13       +3.0*P*P )+U*F13
    *(PI*PI-P*P ))*P/2.0-(4.0*F4  *(4.0*F13       +PI*PI+P*P ))*
    ((2.0*F13       +P*P )**2+P*P *(4.0*F13       +3.0*PI*PI)-U*
    F13       *(PI*PI-P*P ))*PI/2.0)/(((4.0*F13       +PI*PI+P*P
    )**2+4.0*F14       )**2-(4.0*F4  *(4.0*F13       +PI*PI+P*P
    ))**2)
B11=PI/8.0
B20=0.0
B21=-(B2+1.0)*C1*C1
B22=2.*(-.25*PI+B7)*F2*C1
C1=COSF(P/2.0)
C2=COSF(P)
C3=COSF(P/2.0)/(F12       -1.0)
C4=COSF(P/2.0)/((F12       -1.0)*( 9.0*F12       -1.0))
C5=COSF(P)/((PI/P)**2-4.0)
C6=COSF(1.5*P)/(F12       -9.0)
C10=4.0*F31*F32*C1
```

```
      D1= SINF(P/2.0)
      D2=SINF(P)
      D3=SINF(1.5*P)
      D4=SINF(2.0*P)
      D5=SINF(P)/(F12         :.0)
      D6=SINF(P/2.0)/( 4.0*F12      -1.0)
      D10=F31*D1
      D11=F32*D1
      D12=F33*D1
      DX1=2.0*A2/P/F12
      DX2=A2/P/F12/X/X
      DX3=B3/P/F12/X
      DX4=B3*X/F12
      DX5=A2/F12
      DX6=2.0*B3/F12/X
      DX7=1.980/F2/F12/X
      E10=1.0-C2
      E11=D2-P*C2
      E12=(F12+1.0)*C10-P*D12
      E13=F2*D12-F33
      E14=F2*F33-D12
      E15=PI*D12-2.0*F2*C10
      E16=D1-0.5*P*C1
      E17=1.0-C1


C     A2.3 ***** COEFFICIENTS OF ALGEBRAIC EQUATIONS. *****


C     CALCULATION OF C30

      C30=CA30+CB30
C     IN WHICH
      CA30=(A3*A3*PI*F3*P)+2.0*A3*A7*PI*F3   *D2+A7*A7*PI*F3   *(P+D4*0.5)
     1 *0.5-(A3*PI*F13    *(P+D2))*0.25-(A7*PI*F13    *(P*0.5+D2+D4*0.
     2 25))*0.125+(A7*A7*P*F5*(P-D4*.5))*0.25+(A7*B8*F4  *(P-D4*0.5))*
     3 0.5-(A7*F4*P   *(P-D4*0.5))*0.0625+(B8*B8*PI*F3  *(P-D4*0.5))*0
     4 .25-(B8*F3*F4    *(P-D4*0.5))*0.125+(B4*B4*P*P /X*(P+D4*0.5))+B8
     5 *B8*P*P /X*(P+D4*0.5)*0.5+B4*P**3/X*(D2-P*0.5-D4*0.25)*0.5+B8*P
     6 **3/X*0.25 *(D2-P*0.5-D4*0.25)-A7*PI*F13    *(P*0.5+D2+D4*0.25)
     7 *0.125+3.0*PI*F23    /32.0*(0.75*P+D2+D4*.125)+F14      *X*
     8 (P-D4*0.5)/64.0-A7*F4*P   *(P-D4*0.5)*0.0625
```

```
      CB30=0.09375*P**4/X*  (0.75*P-D2+D4*0.125)+
     1 W/V/V *(2.0*A3*A3*PI*F3  +4.0*A3*A7*PI*F3  *C2+2.0*A7*A7*PI*F3
     2    *C2*C2-A3*PI*F13    *C1*C1-A7*PI*F13    *C1*C1*C2+3.0*PI*F23
     3    /8.0*C1**4)+W*Y/V*(4.0*A3*B8*PI*F13    *D1*D1*C1+8.0*A7*B8*PI
     4 *F13    *D1*D1*C1*C2-2.0*B8*PI*F23    *D1*D1*C1**3+4.0*A3*B8*PI*
     5 F13    *D1*D1*C1)+W*Y*Y *(32.0*B8*B8*PI*F23    /3.0*D1**4*C1*C1)

C     CALCULATION OF C21
      C21=CA21+CB21+CC21+CD21+CE21
C     IN WHICH
      CA21=3.0*A3*A5*PI*F2*F3 *C3+3.0*A3*A6*PI*F3  *C3+1.5*A5*A7*PI*F2*
     1 F3*(C3+C6)+1.5*A6*A7*PI*F3  *(3.0*C6-C3)-A3*PI*F2*F13   *C3-A5*
     2 PI*F2*F13   *0.0625*(3.0*C3+C6)-A6*PI*F13    *0.0625*(C3+3.0*C6
     3 )-A7*PI*F2*F13 *0.5  *(C3+C6)+0.375*A5*A7*F4  /X*(C3+3.0*C6)+0.3
     4 75*A5*A7*F4  /X*(C3-C6)-0.375*A6*A7*PI*PI/X*(C3-C6)-0.375*A6*A7
     5 *P*P /X*(C3+3.0*C6)+B8*(A5-A6*F2  )*PI*PI*0.125*(C3-C6)+B8*(A5*
     6 F2  -A6)*F4  *0.125*(C3+3.0*C6)+A7*B9*F4  *(C3+3.0*C6)
     7 +A7*B10*PI*PI*(C3-C6)-(A5*F2  -A6)*0.03125*F4*P   *(C3+3.0*C6)-(
     8 A5-A6*PI/P)*0.03125*PI*F4  *(C3-C6)-A7*PI*F4  *0.25*(C3-C6)
      CB21=-A7*PI*F4  *0.25*(C3+3.0*C6)+1.5*B8*B9*PI*F3  *(C3+3.0*C6)+
     1 1.5*B8*B10*PI*F3*F2 *(C3-C6)+(A5*F2  -A6)*B8*F4  *0.25*(C3+3.0*
     2 C6)+(A5-A6*F2  )*B8*PI*PI*0.25*(C3-C6)+A7*B9*F4  *0.5*(C3+3.0*C6)
     3 +A7*B10*PI**2*0.5*(C3-C6)-(2.0*B8+B10)*0.125*PI**3*X*(C3-C6)-(2.0
     4 *B8*F2  +B9)*0.125*F3*F4    *(C3+3.0*C6)+3.0*B4*B5*P*P /X*((F12
     5    +1.0)*C3+(F12      -3.0)*C6)+6.0*B4*B6*F4  /X*(C3-C6)+1.5*B8*B
     69*P*P /X*((F12      +1.0)*C3+(F12      -3.0)*C6)+3.0*B8*B10*F4  /
     7 X*(C3-C6)+B4*F4*P   /X*(-C3+3.0*C6)+0.125*B5*P**3/X*(F12
     8 3.0)*(C3-C6)+0.25*B6*F4*    F5*(-C3+C6)
      CC21=0.5*B8*F4*F5    *(-C3+3.0*C6)+0.0625*B9*P*P*F5*(F12
     1 -3.0)*(C3-C6)+0.125*B10*F4*F5    *(-C3+C6)-0.125*A5*PI*F13*F2
     2 *(3.0*C3+C6)-0.125*A6*PI*F13    *(C3+3.0*C6)-0.5*A3*PI*F13*F2
     3  *C3-0.25*A7*PI*F13*F2   *(C3+C6)+0.28125*PI*F23*F2   *(3.0*C3+C6
     4 )+PI*F4*F3 *0.03125*(C3-C6)+PI*F4*F3 *0.0625*(C3+3.0*C6)-B10*
     5 PI*PI*F3*.125*(C3-C6)-0.125*(B8*F2  +B9)*F3*F4    *(C3+3.0*C6)-(
     6 A5*F2  -A6)*F4*P   *0.03125*(C3+3.0*C6)-(A5-A6*F2  )*0.03125*PI*F
     7 4  *(C3-C6)-A7*0.125*PI*F4  *(C3+3.0*C6)+0.84375*F4*P*F5  *(C3-C6
     8 )+0.25*B5*P*P*F5*( F12     -3.0)*(C3-C6)
      CD21=0.5*B6*F4*F5    *(-C3+C6)+0.5*B4*F4*F5    *(-C3+3.0*C6)+
     1 0.125*B9*P*P*F5*(F12      -3.0)*(C3-C6)+0.25*B10*F4*F5    *(-
     2 C3+C6)+0.25*B8*F4*F5    *(-C3+3.0*C6)+0.0625*PI*F3*F4 *(C3-C6)+
     3 PI*F3*F4 *0.03125*(C3+3.0*C6)-B9*F3*F4    *0.125*(C3+3.0*C6)-(B8+B
     4 10)*PI**3*X*0.125*(C3-C6)-(A5*F2  -A6)*F4*P   *0.03125*(C3+3.0*C6)
     5 -(A5-A6*F2  )*PI*F4  *0.03125*(C3-C6)-A7*PI*F4  *0.125*(C3-C6)+W/
     6 V/V *(3.0*A3*A6*PI*F3  *D1+3.0*A6*A7*PI*F3  *D1*C2-0.75*A6*PI*F13
     7      *D1*C1*C1)+W*Y/V*(6.0*A3*B9*PI*F13    *D1*C1+6.0*A6*B8*PI*F1
     8 3     *D1**3*C1+6.0*A7*B9*PI*F13    *D1*C1*C2)
```

```
      CE21=W*Y/V*(-1.5*B9*PI*F23     *D1*C1**3)+W*Y*Y *(16.0*B8*B9*PI*F23
     1      *D1**3*C1*C1)

C     CALCULATION OF C12

      C12=CA12+CB12+CC12+CD12+CE12
C     IN WHICH
      CA12=A3*A4*PI*F3*P+0.125*A5*A5*PI*F3  *(P+D2+D5)
     1    +0.125*A6*A6*PI*F3  *(P-D2+D5)+A4*A7*PI*F3  *D2+A7*A7*PI*F3  *
     2 D5-0.125*A3*F13*F4        -0.0625*A5*PI*F13     *(P+D2+D5)-0.0625*A6
     3 *PI* F13*F2  *D5-0.125*A7*PI*F13*F12      *D5+0.015625*A5*A5*PI*F6
     4    *(P+D2-D5)+0.03125*A5*A5*PI*F6  *D5-0.03125*A5*A6*PI*F2*F6 *
     5 D5-0.03125*A5*A6*F4  /X*(P+D2-D5)+0.015625*A5*A5*P*F5  *(P-D2-D5)
     6 -0.03125*A5*A6*F4  /X*(P-D2-D5)-0.03125*A5*A6*F4  /X*D5+0.015625*
     7 A6*A6*PI*F6  *(P-D5-D2)+0.03125*A6*A6*PI*F6  *D5+0.015625*A6*A6*
     8 P*F5  *(P+D2-D5)+0.5*A7*A7*PI*F6  *D5+0.0625*A5*(B9+B10*F2  )*PI
     9 *PI*D5+0.0625*B10*(A5-A6*F2  )*F4  *(P-D2-D5)
      CB12=+0.0625*B9*(A5*F2  -A6)*F4  *(P+D2-D5)-0.0625*A6*(B9*F2  +B
     1 10)*PI*PI*D5+0.5*A7*B11*PI*PI*D5-0.015625*(A5*F2  -A6)*PI*F4  *
     2 D5-0.015625*(A5*F2  -A6)*PI*F4  *(P+D2-D5)-0.015625*(A5-A6*F2  )
     3 *F4*P   *(P-D2-D5)-0.015625*(A5-A6*F2   )*PI**3*D5-0.125*A7*PI**3
     4 *D5+0.25*B9*B9*PI*F3  *(P+D2-D5)+0.25*B10**2*PI*F3  *(P-D2-D5)+0
     5 .5*(B8*B11+B9*B10)*PI*F3*F2 *D5+0.5*A7*B8*PI**3/P*D5+0.0625*(A5*
     6 PI/P-A6)*B9*F4  *(P+D2-D5)+0.0625*((A5*F2  -A6)*B10+(A5-A6*F2  )
     7 *B9)*PI*PI*D5+0.0625*(A5-A6*F2  )*B10*F4  *(P-D2-D5)-0.0625*B9*PI
     8 **3*X*(P+D2-D5)-0.0625*(2.0*B8*F2  +B9+B10*F2  )*PI**3*X*D5
      CC12=-.0625*B10*F3*F4    *(P-D2-D5)+2.0*B4*B7*F4  /X*D5+0.25*B5**
     1 2*P*F5  *((F12      +1.0)*P+(F12      -2.0)*D2)+B5*B6*F4  /X*(P
     2 -0.5*D2)+0.25*B6*B6*P*F5  *((F12      +1.0)*P-F12      *D2)+B8*B
     3 11*F4  /X*D5+0.125*B9*B9*P*F5  *((F12      +1.0)*P+(F12      -2.
     4 0)*D2)+0.5*B9*B10*F4  /X*(P-0.5*D2)+0.125*B10**2*P*F5  *((F12
     5    +1.0)*P-F12      *D2)+0.25*B4*F4*F6    *(D2-D5)-0.125*B5*F4*
     6 F5    *(P-2.0*D2)+0.125*B6*F4*F6    *(D2-P)+0.125*B8*F4*F6    *
     7 (D2-D5)+0.0625*B9*F4*F5    *(2.0*D2-P)+0.0625*B10*F4*F6    *(D2
     8 -P)-0.125*A4*PI*F13    *(P+D2)-0.125*A7*PI*F13    *D5-0.0625*A5*
     9 PI*F13    *(P+D2+D5)-0.0625*A6*PI*F13*F2   *D5
      CD12=0.140625*PI*F23    *(P+D2+D5)+0.03125*PI**4*X*D5+0.015625*PI
     1 **4*X*(P+D2-D5)-0.0625   *B9*PI**3*X*(P+D2-D5)-0.0625*(B10*PI/P+B
     2 11)*PI**3*X*D5-0.0625*A7*PI**3*D5-0.015625*(A5*PI/P-A6)*PI*F4  *
     3 (P+D2-D5)-0.015625*(A5-A6*F2 )*PI**3*D5+0.140625*F14        /X*(P
     4 -D2+D5)-0.25*B7*F4*F5    *D5+0.125*B5*F4*F5    *(2.0*D2-P)+0.125
     5 *B6*F4*F6    *(D2-P)-0.125*B11*F4*F5    *D5+0.0625*B9*F4*F5    *
     6 (2.0*D2-P)+0.0625*B10*F4*F6    *(D2-P)+0.015625*F14        *X*(P-
     7 D2-D5)+0.03125*PI**4*X*D5-0.0625*(B9+B11)*PI**3*X*D5-0.0625*B10*
     8 F3*F4    *(P-D2-D5)-0.0625*A7*PI**3*D5-0.015625*(A5*F2  -A6)*PI*
     9 F4  *D5-0.015625*(A5-A6*F2  )*F4*P   *(P-D2-D5)
```

```
      CG12=W/V/V *(2.0*A3*A4*PI*F3  -2.0*A3*A7*PI*F3  +A6*A6*PI*F3  *D1
     1 *D1+2.0*A4*A7*PI*F3  *C2-2.0*A7**2*PI*F3  *C2-0.5*A4*PI*F13    *
     2 C1*C1+0.5*A7*PI*F13    *C1*C1)+W*Y/V*(2.0*A6*B9*PI*F13    *D1*D1
     3 *C1+4.0*A4*B8*PI*F13    *D1*D1*C1-4.0*A7*B8*PI*F13    *D1*D1*C1+
     4 2.0*A6*B9*PI*F13    *D1*D1*C1)+W*Y*Y *(16.0*B9*B9*PI*F23    /3.0
     5 *D1*D1*C1*C1)    +0.25*A5*A6*PI*F3*F2 *D5
      CE12=A20*(PI*PI*X*(0.375*P-0.25*C2/P)-0.25*P/X*E10+A7/F2/X/X*E10+
     1 B8/X*E10)+B22*(-.5*P*X*E11+.125*P*P*F5*(PI*PI+4.0)/PI/PI*
     2 (P-D2)+A7*2.0/F2*E11+2.0*B8*X*E11+B4*P*F5*D2+4.0*B8/F12/X*D2)

C     CALCULATION OF C03

      C03=CA03+CB03+CC03+CE03
C     IN WHICH
      CA03=A4*A5*PI*F3*F2 *C3+A5*A7*PI*F3*F2 *(12.0*F12      *C4-C3)+A4
     1 *A6*PI*F3  *C3+A6*A7*PI*F3  *(4.0*F12      *C4-C3)-1.5*A5*PI**6*
     2 X**2/P**3*C4-0.5*A6*PI*F13*F12      *C4+0.5*A5*A7*PI*F2*F6    *(3.
     3 0*F12      -1.0)*C4+A5*A7*PI*F2*F6    *C4-A6*A7*PI*F12*F6      *C4
     4 -0.5*A6*A7*PI*F6  *(3.0*F12      -1.0)*C4+B11*(A5-A6*F2  )*PI**3/
     5 P*C4+0.5*B11*(A5*PI/P-A6)*PI*PI*(3.0*F12      -1.0)*C4-0.125*(A5*
     6 F2  -A6)*PI**3*(3.0*F12      -1.0)*C4-0.25*(A5-A6*F2  )*PI**4/P*
     7 C4+2.0*B9*B11*PI*F3*F2 *(3.0*F12      -1.0)*C4+4.0*B10*B11*PI*F3
     8 *F12    *C4+2.0*A7*B9*PI**3/P*(3.0*F12      -1.0)*C4+4.0*A7*B10*P
     9 I*PI*F12 *C4-0.5*B9*PI**4*X/P*(3.0*F12      -1.0)*C4
      CB03=-B10*PI*PI*F3*F12*C4+2.0*B5*B7*F4  /X*(3.0*F12*F12  +6.0*F12
     1       -1.0)*C4+16.0*B6*B7*PI*F12*F6      *C4+B9*B11*F4  /X*(3.0*
     2 F12*F12 +6.0*F12       -1.0)*C4+8.0*B10*B11*PI*F12*F6    *C4+0.5*B
     3 5*F4*F6    *(3.0*F12*F12  -8.0*F12       +1.0)*C4-2.0*B6*PI*PI*F12
     4 *F6*C4+0.25*B9*F4*F6    *(3.0*F12*F12  -8.0*F12       +1.0)*C4-B1
     5 0*PI*PI*F12*F6*C4-0.5*A4*PI*F13*F2    *C3-0.5*A7*PI*F13*F2    *(3.0
     6 *F12       +1.0)*C4+2.25*PI**7*X**3/P**3*C4+0.125*PI**5*X/P*(3.0*
     7 F12      -1.0)*C4-0.5*B11*PI**4*X/P*(3.0*F12       -1.0)*C4-0.5*A
     8 7*PI**4/P*(3.0*F12       -1.0)*C4+0.375*PI*F4*F6 *(7.0*F12       -
     9 1.0)*C4+B7*F4*F6    *(4.0*F12       *C4-C3)
      CC03=0.5*B11*F4*F6    *(4.0*F12       *C4-C3)+0.25*PI**5*X/P*C4-B1
     1 1*PI**4*X/P*C4-A7*PI**4/P*C4+W/V/V *(A4*A6*PI*F3  *D1-A6*A7*PI*F
     2 3  *D1)+W*Y/V*(2.0*A4*B9*PI*F13    *D1*C1-2.0*A7*B9*PI*F13    *D
     3 1*C1)
      CE03=A20*(2.0*F3*F2*(F31+D11+F32-D10)-F6*E14-F5*E13+A5/X/X*E14+
     1 A5/F2/X/X*E13-A6/X/X*E13-A6/F2/X/X*E14+B9*4.0/X*E14+4.0*B10/
     2 X*E13)+B22*(-2.0*F3*E12+0.5*F5/F2*(PI*PI+4.0)*C3-2.0*P*X*E15
     3 +A5*2.0*E12+A5*2.0*(P*D12-2.0*C10)-A6*2.0*E15-2.0*A6/F2*E12+
     4 8.0*B9*X*E12+8.0*B10*X*E15+B5*P*F5*(F12-1.0)*C3+4.0*B9/F12/X
     5 *(F12-1.0)*C3)
```

```
C     CALCULATION OF C20

      C20=CA20+CB20+CE20
C     IN WHICH
      CA20=1.0/Y*(4.0*A1*A3*F3  *D1+2.0*A1*A7*F3  *(D1+D3/3.0)+A1*F13
     1    *0.5*(3.0*D1+D3/3.0)+   2.0*A1*A7*F5/F2    *(D1-D3/3.0)
     2 +2.0/3.0*A1*B8*P*(3.0*D1-D3)+2.0
     3 *A7*B2*P*(D1-D3/3.)-1.0/6.0*A1*P*P *(3.0*D1-D3)+2.0/3.0*B2*B8
     4 *F3  *(3.0*D1-D3)
     5 -1.0/6.0*B2*F4  *X*(3.0*D1-D3)+6.0*B2*B4*F5/F2    *(D1
     6 +D3/3.0)+2.0*B2*B8*F5/F2    *(D1+D3/3.0)+6.0*B4*F5/F2    *(D1+D3
     7 /3.0)+2.0*B8*F5/F2    *(D1+D3/3.0)+B2/3.0*P*F5/F2  *(3.0*D1-D3)+
     8 P*F5/3.0/F2  *(3.0*D1-D3))+W/Y/V/V *(4.0*A1*A3*F3  *C1+4.0*A1*A7
     9 *F3  *C1*C2+2.0*A1*F13        *C1**3)
      CB20=W/V*(-2.0*A3*F13      *C1*C1-2.0*A7*F13       *C1*C1*C2+8.0
     1 *A1*B8*F13        *D1*D1*C1*C1+2.0*A3*B2*F13       *D1*D1+2.0*A7*
     2 B2*F13         *D1*D1*C2-F23        *C1**4+B2*F23        *D1*D1*C1*C
     3 1)+W*Y*(-16.0/3.0*B8*F23         *D1*D1*C1**3+16.0/3.0*B2*B8*F23
     4     *D1**4*C1)
      CE20=4.0/Y*(B21*(B8*0.75*X*E11+A7*0.75/F2*E11-3.0/16.0*P*X*E11+
     1 B4*0.5*P*P/X*D2+1.5*B8/F12/X*D2+1.0/16.0*P*(PI*PI+3.0)/F12/
     2 X*(P-D2)))


C     CALCULATION OF C11

      C11=CA11+CB11+CC11+CE11
C     IN WHICH
      CA11=1.0/Y*(4.0/3.0*A1*A5*X*P*(1.0+C2+4.0*C5)+8.0/3.0*A1*A6*PI*X*
     1 C5+8.0/3.0*A2*A3*X*P+8.0/3.0*A2*A7*F3*F2     *C5+4.0/3.0*A1*PI*P*
     2 X*X *(1.0+C2+4.0*C5)+4.0/3.0*A1*A5*P/X*C5+2.0/3.0*A1*A5*P/X*(1./
     3 F12    -C5)-2.0/3.0*A1*A6*PI/X*(1./F12    -C5)-4.0/3.0*A1*A6*P*P/
     4 PI/X*C5+16.0/3.0*A2*A7*P/X*C5+8.0/3.0*A1*B9*P*C5+8.0/3.0*A1*B10*
     5 PI*(1./F12    -C5)+B2*(A5-A6*PI/P)*PI/3.0*(1./F12    -C5)+2.0/3.0*
     6 B2*(A5*PI/P-A6)*P*C5+16.0/3.0*A7*B3*P*C5-2.0/3.0*A1*PI*P*(1./F12
     7    -C5)-2.0/3.0*A1*PI*P*C5+16.0/3.0*B2*B9*PI*X*C5+8.0/3.0*B2*B10
     8 *F3*F2     *(1./F12    -C5)+16.0/3.0*B3*B8*PI*X*C5+2.0/3.0*B2*(A5*
     9 PI/P-A6)*P*C5+B2*(A5-A6*PI/P)*PI/3.0*(1./F12    -C5))
      CB11=1.0/Y*(8.0/3.0*(2.0*A2*B8*PI/P+A1*B9)*P*C5-2.0/3.0*B2*PI*F3
     1  *C5-2.0/3.0*B2*PI*F3  *(1./F12    -C5)+8.0*B3*B4*PI/X*C5+4.0*B2*
     2 B5*F5/F2     *(1.0+C2+2.0*C5)+4.0*B2*B6*F5/F12       *(1.0+C2+(4.0
     3 -2.0*F12         )*C5)+4.0/3.0*B2*B9*F5/F2.    *(1.0+C2+2.0*C5)+4.0/
     4 3.0*B2*B10*F5/F12        *(1.0+C2+(4.0-2.0*F12         )*C5)+8.0/3.0*
     5 B3*B8*PI/X*C5+8.0*B4*P/X*C5+4.0*B5*F5/F2       *(1.0+C2+2.0*C5)+4.0
     6 *B6*F5/F12        *(1.0+C2+(4.0-2.0*F12         )*C5)+8.0/3.0*B8*P/X*
     7 C5+4.0/3.0*B9*F5/F2      *(1.0+C2+2.0*C5)+4.0/3.0*B10*F5/F12
     8 *(1.0+C2+(4.0-2.0*F12         )*C5)+16.0/3.0*B2*P*F5  *C5+16.0/3.0*
     9 P*F5  *C5+2.0/3.0*A2*PI*P*X*X *(1.0+C2+4.0*C5))
```

```
      CC11=1.0/Y*(-2.0/3.0*(B2*PI/P+B3)*PI*P*X*C5-2.0/3.0*(A1+A2)*PI*P*C5
     1 +4.0/3.0*B3*PI*P/X*(1./F12   -C5)+4.0/3.0*P*F5  *(1./F12   -C5)
     2   -2.0/3.0*B3*PI*P*X*C5-2.0/3.0*A2*PI*P*C5)+W/Y/V/V *(8.0/3.0*A1
     3 *A6*PI*X*D1*C1)+W/V*(-4.0/3.0*A6*F13         *D1*C1*C1+16.0/3.0*A1
     4 *B9*F13         *D1*C1*C1+4.0/3.0*A3*B3*F13         *D1+4.0/3.0*A6*B
     5 2*F13        *D1**3+4.0/3.0*A7*B3*F13         *D1*C2+2.0/3.0*B3*F23
     6        *D1*C1*C1)+W*Y*(-32.0/9.0*B9*F23         *D1*C1**3+32.0/9.0*B
     7 2*B9*F23         *D1**3*C1+32.0/9.0*B3*B8*F23         *D1**3*C1)
      CE11=B21*4./Y*(4.0*B9*X*E12+4.0*B10*X*E15+A5*E12+A5*(P*D12-2.*C10)
     1 -A6*E15-A6/F2*E12+B5*2.0/3.0*P*F5*(F12-1.0)*C3+2.0*B9/X*(
     2 1.0-1.0/F12)*C3+1.0/3.0/F2*F5*(PI*PI+3.0)*C3+F3*(1.0-F12)
     3 *C10)

C     CALCULATION OF CO2

      CO2=CA02+CB02+CC02+CE02
C     IN WHICH
      CA02=1.0/Y*(4.0/3.0*A1*A4*F3  *D1+4.0/3.0*A1*A7*F3  *D6+8.0/3.0*A2
     1 *A5*F3*F12        *D6+4.0/3.0*A2*A6*F2*F3     *D6+4.0/3.0*A1*F13*F12
     2           *D6+8.0/3.0*A1*A7*F6  *D6+1.0/3.0*A2*A5*F6  *(D1-D6)+2
     3 .0/3.0*A2*A5*F6  *D6-2.0/3.0*A2*A6*F2*F6     *D6-1.0/3.0*A2*A6*F5
     4   *(D1-D6)+8.0/3.0*A1*B11*PI*D6+1.0/3.0*B3*(A5*F2  -A6)*P*(D1-D
     5 6)+2.0/3.0*B3*(A5-A6*F2  )*PI*D6-2.0/3.0*A1*PI*PI*D6+4.0/3.0*B3
     6 *B9*F3  *(D1-D6)+8.0/3.0*(B2*B11+B3*B10)*F3*F2    *D6+8.0/3.0*A
     7 7*B2*PI*F2  *D6+4.0/3.0*A2*B9*PI*(D1-D6)+8.0/3.0*A2*B10*PI*F2
     8 *D6-2.0/3.0*B2*PI*F3*F2 *D6+4.0*B3*B5*F6  *(2.0*F12      -1.0)*
     9 D6+4.0*B3*B6*F2*F6    *D6+4.0*B2*B7*F5 *D6+4.0/3.0*B2*B11*F5 *D6)
      CB02=1.0/Y*(4.0/3.0*B3*B9*F6  *(2.0*F12       -1.0)*D6+4.0/3.0*B3
     1 *B10*F2*F6    *D6+4.0*B5*F5 *(2.0*F12      -1.0)*D6+4.0*B6*F6
     2 *D6+4.0/3.0*B9*F5 *(2.0*F12       -1.0)*D6+4.0/3.0*B10*F6   *D6+2
     3 .0/3.0*B2*F4  /X*(D1-D6)+4.0*B7*F5 *D6+4.0/3.0*B11*F5 *D6+2.0/3
     4 .0*F4  /X*(D1-D6)+8.0/3.0*A2*F13*F12          *D6-B3/3.0*PI*F3  *
     5 (D1-D6)-A2/3.0*PI*PI*(D1-D6)+8.0/3.0*B3*PI*F6  *D6+8.0/3.0*F4
     6 /X*D6-2.0/3.0*B3*PI*F3  *D6-2.0/3.0*A2*PI*PI*D6)+W/Y/V/V *(4.0/
     7 3.0*A1*A4*F3  *C1-4.0/3.0*A1*A7*F3  *C1)+W/V*(2.0/3.0*A6*B3*F13
     8         *D1*D1-2.0/3.0*A4*F13        *C1*C1+2.0/3.0*A7*F13       *C
     9 1*C1+2.0/3.0*F13*D1*D1   *B2*(A4-A7))
      CC02=W*Y*(16.0/9.0*B3*B9*F23         *D1*D1*C1)
      CE02=1.0/Y*(B21*(B11*P*X/F2+A7*P/F2-0.25*P*P*X+P*P/12.0/X* (PI*PI+
     1 3.0))+8.0*B22/F12/X*D1+A20*A1*E17*(8./P+4.0*P/F13)+B22*E16*(A
     2 1/F2+B2*X)*4.0+B21*B22/6.0*P*P*P*X+A20*B2*4.0/F3*E17+A20*B21/6.0
     3 *P*F5+B2*B22*8.0/F12/X*D1+B21*B22*5.0/12.0*P*P*F5)
```

```
C       CALCULATION OF D03

        D03=D03 +DE03
C       IN WHICH
        D03=A4*A4*PI*F3*P+0.5*A7*A7*F3*F4     -0.125*A4*F4*F13       -0.0
      1 625*A7*F4*F13        +0.25*A7*A7*F4*F6     +0.25*A7*B11*PI*F4  -0.
      2 0625*A7*PI**3*P+0.25*B11*B11*F3*F4    +0.25*A7*B11*PI*F4  -0.0625
      3 *B11*PI*F3*F4 +B7*B7*F4*F6     +0.5*B11**2*F4*F6     -0.125*B7*PI*
      4 F4*F6 -0.0625*B11*PI*F4*F6 -0.125*A4*F4*F13         -0.0625*A7*
      5 F4*F13  +0.0703125*F4*F23         +0.0078125*PI**4*P*X-0.03125*B11
      6 *PI*F3*F4 -0.03125*A7*PI**3*P+0.0703125*PI**4*P/X-0.125*B7*PI*F4
      7 *F6   -0.0625*B11*PI*F4*F6 +0.0078125*PI**4*P*X-0.03125*B11*PI*F3
      8 *F4   -0.03125*A7*PI**3*P+W/V/V *(2.0*A4*A4*PI*F3  -4.0*A4*A7*PI
      9 *F3   +2.0*A7*A7*PI*F3)
        DE03=2.0*(A20*(1./3.0*A20*P/X+PI*PI*X*(0.125*P+0.5/P/F12)+2.0*A7/
      1     F2/X/X+2.0*B11/F2/X-0.5*P/X)+B22*(2.0*B11*P*X/F2+2.0*A7*P/F2
      2     -0.5*P*P*X+0.125*P*P/X*(PI*PI+4.0))+A20*(A20*P/6./X/X/X+B22
      3     *0.25*F5*P)+B22*B22*P*P*P/3.0*(X/2.0+1.0/X))


C       CALCULATION OF D02

        D02=D02N+DE021+DE022
C       IN WHICH
        D02N=1.0/Y*(4.0*A2*A4*P*X+4.0/3.0*A2*A7*P*X+4.0/9.*A2*F4*X*X
      1 +8.0/3.0*A2*A7*P/X+8.0/9.0*A2*B11*P+16.0/9.0*A7*B3*P-2.0/9.0*A2
      2 *F4   +8.0/9.0*B3*B11*         P*X+16.0/9.0*B3*B11*P*X+8.0/9.0*A
      3 7*B3*P+16.0/3.0*A2*B11*P-2.0/9.0*B3*F3  *P+4.0*B3*B7*P/X+4.0/3.0
      4 *B3*B11*P/X+8.0/3.0*B7*F5/F2     +8.0/9.0*B11*F5/F2     +4.0/9.0*
      5 B3*F4  /X+4.0/3.0*B7*F5/F2     +4.0/9.0*B11*F5/F2     +4.0/9.0*P*
      6 F5   +8.0/9.0*A2*F3*P*X    -2.0/9.0*B3*F4   *X-2.0/9.0*A2*F4   +8.0
      7 /9.0*B3*F4   /X+8.0/9.0*P*F5   -2.0/9.0*B3*F4   *X-2.0/9.0*A2*F4    )
      8 +W/V*(2.0*A4*B3*F13          *D1-2.0*A7*B3*F13          *D1)
        DE021=12./Y*B22*(DX4+DX5+DX6+DX7)
        DE022=12.0/Y*(DX1+DX2+DX3)*A20
C       CALCULATION OF C10

        C10=CA10+CB10+CE10
C       IN WHICH
        CA10=1.0/Y/Y *(A1*A1*PI*F3  /4.0*(P+D2)+A1*A1*P*F5*.125    *(P-D2)+
      1  A1*B2*F4  /8.0*(P-D2)+B2*B2*PI*F3*.1250*(P-D2)+0.125*A1*B2*F4
      2  *(P-D2)+2.0*Q*B4*P*F5  *(D1+D3/3.0)+B2*P*F5*.5      *(P+D2)+P*F5
      3  *.25     *(P+D2)+.25*B2*B2*P*F5 *(P+D2)+Q*P**3/(12.0*X)*(3.0*D1-
      4  D3))+1.0/12.0*(0.25*PI*F23      *(P+D2)+0.25*P**4/X*(P+D2)+0.5*F14
      5          *X*(P-D2))+W/(Y*Y *V*V )*A1*A1*PI*F3  *C1*C1+W/(Y*V)*(-
      6  0.5*A1*PI*F13     *C1**3+0.5*A1*B2*PI*F13      *D1*D1*C1-0.5*A1*PI
      7  *F13      *C1**3+0.5*A1*B2*PI*F13      *D1*D1*C1)+W*(PI*F23     /3.0*
      8  C1**4-2.0*B2*PI*F23     /3.0*D1*D1*C1*C1)
```

```
      CB10=W*(B2*B2*PI*F23    /3.0*D1**4)-Q*Z*Z /144.0*B4/(3.0*X)*(3.0*
     1 D1-D3)
      CE10=4.0/Y/Y*(B21*(B2*8.0*X/PI*E16+A1*8.0*P/PI/PI*E16+(16.0/F12/
     1     F3*D1)*(B2+1.0)+B21*P*P*P*X/18.0+B21*P*P*P/X*2.0/15.0)+B20*
     2     P*P*P/16.0/X*(P-D2)+B4*B20*0.5*P*P/X*D2)


C     CALCULATION OF C01

      C01=C01 +CE01
C     IN WHICH
      C01 =1.0/Y/Y *(A1*A2*PI*F3*F2 *C3+0.5*A1*A2*F4  /X*C3+0.5*A1*B3*
     1 F4  *C3+0.5*B2*B3*PI*F3  *C3+0.5*A2*B2*PI*PI*C3+Q*B5*P*F5  *(1.0
     2 +C2+2.0*C5)+Q*B6*P*F5/F2    *(1.0+C2+(4.0-2.0*F12      )*C5)+B2
     3 *B3*PI*F6  *C3+B2*F4  /X*C3+F4  /X*C3+B3*PI*F6  *C3+Q*F4*F5
     4 *C5)+1.0/12.0*(PI*F23*F2   *C3+PI*F4*F6 *C3+2.0*PI*F3*F4 *C3)+
     5 W/(Y*V)*(0.5*A1*B3*PI*F13    *D1*C1)+W*(-B3*PI*F23    /3.0*D1*
     6 C1*C1+B2*B3*PI*F23    /3.0*D1**3)-Q*Z*Z /144.0*(2.0*B5/X*C5+B6
     7 *P/F3    *(1.0-F12       *C5))
      CE01=4.0/Y/Y*(B21*(B3*4.0*X/PI/F12+A2*4.0/F12/PI+B3*8.0/F12/F3+8.0
     1 *P/PI/F12/F3)+B20*0.25*PI*P*F5*C3+B5*B20*P*P/X*0.5*(F12-1.0)*
     2 C3)


C     CALCULATION OF C00

      C00=QR/Y**4*4.0/F3*D1


C     CALCULATION OF D01

      D01= D01 +DE01
C     IN WHICH
      D01=1.0/Y/Y *(0.25*A2*A2*F3*F4    +0.125*A2*A2*F4*F6    +0.25*A2
     1 *B3*PI*F4  +0.125*B3*B3*F4*F3    +4.0*Q*B7*F4  /X*D6+0.25*B3*B3
     2 *F4*F6     +0.5*B3*F4*F5     +0.25*P**3/X+0.5*Q*F4*F6    *(D1-D6))
     3 +1.0/12.0*(0.25*F4*F23       +0.25*PI*PI*F4*(F6+2.*F3))    +W*B3*
     4 B3*PI*F23    /3.0*D1*D1-Q*Z*Z /144.0*4.0*B7*PI/(P*X)*D6
      DE01=1.0/Y/Y*(Q*B22*P*P*F5*C1+0.25 *B20*F14/X+B20*B22    *F5*P*P)


C     CALCULATION OF D00

      D00 =4.0/Y/Y/Y*(B20*P/F12/X+B20*B3/F2*F5 )+QR/Y**4*4.0/F2/F3
```